

# The Design of Novel Functional Materials Based on Cellulose Nanocrystals/Nanofibrils

by

Yang Song

A thesis  
presented to the University of Waterloo  
in fulfillment of the  
thesis requirements for the degree of  
Master of Applied Science  
in  
Chemical Engineering

Waterloo, Ontario, Canada, 2015

© Yang Song 2015

## ABSTRACT

As the most abundant organic biomass on the planet, cellulose provides environmental, biocompatible and sustainable benefits. When treated by acid hydrolysis, highly crystalline nano-rods, called cellulose nanocrystals (CNCs), are generated. Besides the characteristics inherited from natural raw cellulose, this defect-free residue also displays unsurpassed physical properties, such as high tensile strength and ultrahigh specific surface area. The combination of these features makes CNC an excellent candidate for composite materials and building blocks. A partially sulfate esterified surface endows CNC aqueous suspensions with further properties. Dispersions of CNC with this modification are more stable and the abundant hydroxyl groups allow for various kinds of chemical modifications and polymer grafting. Another by-product of cellulose, called cellulose nanofibrils (CNFs), is produced through mechanical disintegration. CNFs have a lower crystallinity than CNCs and they deserve attention due to their flexibility, compressibility and ductility. It is well-known that CNF based foam possesses many attractive features, such as being ultralight, low-cost and ease of preparation. This kind of 3D structure with superior mechanical performance has potential applications in a broad range of fields.

Carbon based materials, like graphene and fullerene, are used in a wide variety of applications due to their outstanding properties. For example, graphene enhanced supercapacitors and fullerene supported anti-oxidant agents are both attracting increasing attention. However, the inherent  $\pi$ - $\pi$  stacking phenomenon hinders their processability in water, making them less environmentally friendly in design and manufacturing. The

emergence of nanotechnology has offered an alternative-method of processing carbon based materials in aqueous phase, supporting their inclusion in environmentally friendly materials.

This study involves the combination of fullerene and CNC to design an aqueous system with a high stability and free-radical scavenging properties. Both physical and chemical interactions between fullerene and CNC will be examined for their long-term stability. The morphology and structure of the system will be investigated and the conditions of synthesis will be optimized. Another focus is to incorporate CNF for the preparation of three-dimensional foam/aerogel with outstanding mechanical properties for waste water treatment. Non-toxic and water-soluble cross-linking agent ethylenediamine, will be used to form and enhance the mechanical properties of the structure. They will also confer chemically domains or grafting anchors on the inner and outer surface of the structure. CNF based foam could have compressible and twistable morphologies, both of which make it applicable to wearable/portable electronic devices. Porous 3D foam with a highly reactive surface could be able to coordinate with metal ions or bind with metal nanoparticles. Thus, CNF aerogels could be used to treat waste water contaminated with heavy metals and as a catalyst support or matrix for various metal oxide nanoparticles.

## **AUTHOR'S DECLARATION**

I hereby declare that I am the sole author of this thesis. This is a true copy of the thesis, including any required final revisions, as accepted by my examiners.

I understand that my thesis may be made electronically available to the public.

## **ACKNOWLEDGEMENTS**

Firstly, I would like to express my sincerest gratitude towards my supervisor, Professor Michael K.C. Tam, for his constant support, inspirational guidance and academic feedback throughout my time in the laboratory.

I would also like to thank the members of my committee, Dr. Juewen Liu and Dr. Michael Pope, for their insightful comments and constructive criticisms. Their guidance helped to improve the quality of this thesis.

I would also like to extend my genuine appreciation to Dr. Holger Kleinke and Dr. Juewen Liu for allowing me to access their instruments for some additional characterizations needed in my research. Pyrolysis and carbonization was performed using Dr. Kleinke's tube furnace and zeta potential analysis was determined using Dr. Liu's Malvern Nano ZS Zetasizer DLS system.

Also, special thanks to all of my lab mates and visiting researchers who made the past two years such an unforgettable experience. Thank you for their open-minded instructions and constructive discussions throughout my studies.

Lastly, I would like to thank my parents, family and friends for being an immense source for inspiration, generosity and love.

## TABLE OF CONTENTS

CHAPTER 1 - Introduction .....	1
1.1 Background information on cosmetics.....	2
1.1.1 The history of cosmetics .....	2
1.1.2 Cosmetic ingredients.....	3
1.1.3 Purposes and meanings of cosmetics .....	4
1.2 Background information on water pollution .....	6
1.2.1 Heavy metal pollution.....	6
1.2.2 Other pollution sources.....	7
1.2.3 Pollution control methods.....	8
1.3 Research scope.....	10
1.4 Thesis outline.....	11
CHAPTER 2 - Literature review.....	12
2.1 Water-soluble fullerene and its derivatives .....	13
2.1.1 Host-guest interactions .....	13
2.1.2 Polymer-fullerene systems .....	14
2.1.3 Other types of water-soluble fullerenes .....	17
2.2 Surface modifications of cellulose nanocrystals (CNCs).....	20
2.2.1 Non-covalent modification methods.....	20
2.2.2 Covalent modification methods .....	22
2.2.2.1 Surface group conversion and substitution.....	22

2.2.2.2 The “graft from” method .....	23
2.2.2.3 The “graft onto” method.....	25
 CHAPTER 3 - The preparation of poly(2-hydroxyethyl methacrylate)-cellulose nanocrystals grafted fullerene (pHEMA-CNC-g-C <sub>60</sub> ) and its anti-oxidant property .....	 28
3.1 Introduction .....	29
3.2 Experimental section .....	32
3.2.1 Materials.....	32
3.2.2 Methods .....	32
3.2.2.1 Synthesis of pHEMA-CNC.....	32
3.2.2.2 Synthesis of pHEMA-CNC-g-C <sub>60</sub> .....	32
3.2.2.3 The protocol of anti-oxidant test.....	33
3.3 Characterizations .....	35
3.3.1 The mechanisms of synthesis .....	35
3.3.2 Fourier Transformation Infrared Spectroscopy (FT-IR).....	37
3.3.3 Proton Nuclear Magnetic Resonance ( <sup>1</sup> H-NMR).....	38
3.3.4 Thermal Gravimetric Analysis (TGA).....	40
3.3.5 The anti-oxidant property.....	41
3.4 Conclusions.....	44
 CHAPTER 4 - The theory of adsorption.....	 45
4.1 Overview of adsorption .....	46
4.2 Modes of adsorption .....	48
4.2.1 Physical adsorption.....	48

4.2.2 Chemical adsorption.....	49
4.2.3 Electrostatic adsorption.....	50
4.3 Equilibrium adsorption isotherms .....	51
4.3.1 Langmuir model .....	51
4.3.2 Freundlich model and Temkin model.....	53
4.4 Adsorption kinetics .....	54
 CHAPTER 5 - Cellulose nanofibrils (CNFs) based aerogels as adsorbents to treat waste water .....	 57
5.1 Introduction .....	58
5.2 Experimental section .....	61
5.2.1 Materials.....	61
5.2.2 Methods .....	61
5.2.2.1 Synthesis of polydopamine-CNF (PDA-CNF).....	61
5.2.2.2 Synthesis of CNF based aerogels .....	62
5.3 Characterizations .....	63
5.3.1 The mechanisms of synthesis .....	63
5.3.2 Fourier Transformation Infrared Spectroscopy (FT-IR).....	66
5.3.3 The optimization of CNF based aerogels .....	67
5.3.4 The removal of methyl orange (MO) .....	69
5.3.4.1 Kinetic study of MO adsorption.....	70
5.3.4.2 Equilibrium adsorption of MO .....	73
5.3.4.3 The effects of pH on MO adsorption.....	75
5.3.5 The removal of Cu <sup>2+</sup> .....	76



5.3.5.1 Kinetic study of Cu <sup>2+</sup> adsorption.....	77
5.3.5.2 Equilibrium adsorption .....	79
5.3.5.3 The effects of pH on Cu <sup>2+</sup> adsorption.....	81
5.4 Conclusions.....	82
CHAPTER 6 - Conclusions and recommendations for future study .....	84
6.1 Conclusions for the study presented in chapter 3.....	85
6.2 Conclusions for the study presented in chapter 5.....	87
6.3 Recommendations for future study relevant to the work in chapter 3 .....	90
6.4 Recommendations for future study relevant to the work in chapter 5 .....	91
References .....	93

## LIST OF FIGURES

<b>Figure 1.1</b> General ingredients of cosmetics .....	5
<b>Figure 1.2</b> The accumulation of pollutants in the food chains .....	9
<b>Figure 2.1</b> Structures of fullerene-containing polymers.....	15
<b>Figure 2.2</b> Surface conversion and substitution of CNC.....	23
<b>Figure 3.1</b> The morphology of cellulose nanocrystals .....	31
<b>Figure 3.2</b> FTIR spectra of CNC, pHEMA-CNC and pHEMA-CNC-g-C <sub>60</sub> .....	37
<b>Figure 3.3</b> <sup>1</sup> H-NMR spectrum of pHEMA-CNC-g-C <sub>60</sub> .....	38
<b>Figure 3.4</b> TGA profile of C <sub>60</sub> , pHEMA-CNC and pHEMA-CNC-g-C <sub>60</sub> .....	40
<b>Figure 3.5</b> Time dependent UV-vis spectra for the oxidation of DPPH .....	41
<b>Figure 3.6</b> The kinetic curve of free radical scavenging .....	43
<b>Figure 4.1</b> The mass transfer between adsorbates and adsorbents .....	46
<b>Figure 4.2</b> Lennard-Jones potential .....	48
<b>Figure 5.1</b> Chemical structure of (a) DOPA and (b) Dopamine.....	63
<b>Figure 5.2</b> The cross-linking reaction between PEI and PDA.....	65
<b>Figure 5.3</b> FTIR spectra of the composite aerogels.....	66
<b>Figure 5.4</b> CNF aerogels with compressible performances.....	68
<b>Figure 5.5</b> The calibration curve of MO.....	69

<b>Figure 5.6</b> The kinetic study of MO adsorption .....	70
<b>Figure 5.7</b> The linearized plot for adsorption of MO onto CNF aerogels .....	74
<b>Figure 5.8</b> The effects of pH on the adsorption of MO onto CNF aerogels .....	75
<b>Figure 5.9</b> The calibration curve of Cu <sup>2+</sup> /ethylenediamine complex .....	76
<b>Figure 5.10</b> The kinetic study of Cu <sup>2+</sup> adsorption .....	77
<b>Figure 5.12</b> The effects of pH on the adsorption of Cu <sup>2+</sup> onto CNF aerogels.....	81

## LIST OF TABLES

<b>Table 1.1</b> The effects of heavy metals and Maximum Contaminant Level .....	7
<b>Table 2.1</b> Solubility of different CD/C <sub>60</sub> complexes .....	14
<b>Table 2.2</b> Summary of water-soluble fullerene polymeric systems .....	16
<b>Table 4.1</b> Physical adsorption vs Chemical adsorption .....	50
<b>Table 4.2</b> Freundlich isotherm vs Temkin isotherm .....	53
<b>Table 4.3</b> Kinetics models of adsorption .....	56
<b>Table 5.1</b> CNF aerogels with different amounts of PDA-CNF .....	67
<b>Table 5.2</b> CNF aerogels with different concentration of PEI .....	68
<b>Table 5.3</b> Parameters in pseudo 2 <sup>nd</sup> order model and intra-particle model .....	72
<b>Table 5.4</b> Parameters in pseudo 2 <sup>nd</sup> order model and intra-particle model .....	79
<b>Table 5.5</b> Different kinds of biomass based adsorbent for the removal of Cu <sup>2+</sup> .....	83
<b>Table 5.6</b> Different kinds of biomass based adsorbent for the removal of MO .....	83

## LIST OF SCHEME

<b>Scheme 2.1</b> The synthesis of $\beta$ -CD/C <sub>60</sub> complex .....	14
<b>Scheme 2.2</b> The synthetic route of fullerol.....	17
<b>Scheme 2.3</b> The synthesis of hyaluronated fullerenes .....	18
<b>Scheme 2.4</b> The fabrication of CNC@polyrhodanine core-shell nanoparticles .....	21
<b>Scheme 2.4</b> The mechanism of CAN to activate cellulose.....	24
<b>Scheme 2.5</b> The design of duplexed DNA-g-CNC.....	26
<b>Scheme 2.6</b> Common polymers used in chemical grafting method.....	27
<b>Scheme 3.1</b> The overall process to synthesize pHEMA-CNC-g-C <sub>60</sub> .....	36
<b>Scheme 5.1</b> The preparation of CNF based aerogels .....	62

# CHAPTER 1

## Introduction

---

## **1.1 Background information on cosmetics**

### **1.1.1 The history of cosmetics**

Dated to over five thousand years ago, Sumerian people from the south part of Mesopotamia invented the first “lipstick” by grounding gemstones. This kind of mineral powders were used to decorate their faces, mainly on the lips and eyelids (Schaffer 2007). Meanwhile, women in the Indus valley were using red dyes extracted from algin as makeups to paint their faces and bodies (Marcus 2009). Ever since then, the trend of extracting colorful dyes from nature for use as paints and decorative elements took place across ancient civilizations (Johnson 1999). For examples, tinted or colored dyes extracted from algae and they were used ancient Phoenicia people to resist dryness (Johnson 1999). Likewise, ancient civilizations like ancient China, also applied natural derivatives to increase moisture retention in the skin, to smooth frown lines on the forehead and to prevent senile degradation of micro-blood vessels (Witkowski and Parish 2001). In ancient Japan, a frond-like and gelatinous basidiocarps, called tremella fuciformis, was used to enhance anti-ageing effects because of the presence of superoxide dismutase (Hyde, et al. 2010).

However, those kinds of primitive and underdeveloped extraction or concentration processes may cause serious diseases due to a high content of halogen and other toxic compounds (Reshetnikov, et al. 2000). Even in the period known as the Age of Enlightenment, most men and women were blindly using poorly refined makeups to follow a so-called fashion (Parry and Eaton 1991). The widespread use of such powders that may

contain high level of toxic metals and other poisonous compounds led to a series of chronic symptoms (Witkowski and Parish 2001).

In the late 16<sup>th</sup> century, a huge demand from upper class women who were using makeups initiated the commercialization of cosmetics and accelerated its prosperity (Romm 1989). Later on, the cosmetics market was expanding exponentially since L'Oréal, the largest cosmetics company, gradually built a globally connected marketing network around the 19<sup>th</sup> century (Balmer, et al. 2007). In the modern age, with the emergence of versatile types of cosmetics, including lotion, perfume, fingernail, skin-care cream, the products are being comprehensively specialized to enhance the appearance as well as to protect the complexion of human body (Groot 1987). Although it was common for ladies to use cosmetics daily, body protection cosmetic products also have the potential to be popularized among men, improving their appearance and body odor.

### **1.1.2 Cosmetic ingredients**

Generally speaking, the ingredients of typical cosmetics can be divided into two groups, natural organics and mineral inorganics. Modified natural oils, like coconuts oils, are extremely popular in some tropical regions because of their excellent performance in moisture retaining and skin smoothing (Cope 2003) (Lynde 2001). Vibrant dyes extracted from crushed insects or colorful foliage are also found in many cosmetics, labelled as natural essences (Siva 2007). Unlike organic ingredients, mineral inorganics usually contain no artificial odor, synthetic preservative and chemical dye. For instance, pearl powders are widely used to improve the appearance of skins by giving them a nacreous or



sparkling luster (Nagatani, et al. 2002). Another common source of gloss effects comes from natural mineral mica which is coated by a thin layer of titanium dioxide (Topuz, et al. 2011). In this approach, the color could be changed by varying the thickness of shell-layer.

In summary, cosmetics are mainly comprised of three factors: fragrant odor, visual effect and functional element. Fragrance and must be combined with the functionality of the cosmetics. Because the ultimate purpose of using makeups is to cover and conceal imperfections, or even naturally slow down the aging process. Hence, the anti-aging performance and anti-oxidant property are the most common selling points in cosmetics market nowadays (Kumar 2005).

### **1.1.3 Purposes and meanings of cosmetics**

The primary purpose of using cosmetics is to protect human bodies from the natural elements, including sunlight, wind, dryness and heat. As the evidence discovered by archaeologist, people in the early Stone Age painted themselves with clay or mixtures of plant saps to protect their skin against the burns from sunlight and the fissures in the skin caused by cold winds (Leung and Foster 1996) (Aburjai and Natsheh 2003). However, since human society progressed into the age of enlightenment, the demands for cosmetics have broadened extensively, not only for basic functions like body protection, but also for personal hygiene and attractiveness (Chaudhri and Jain 2009). The damages caused by environmental impacts were significantly decreased due to a better living condition and improved quality of diet. Especially after the industrial revolution, the immensely expanded manufacturing provided people with richness in every aspect of their daily lives. Just like

the Hierarchy of Needs theory proposed by Malsow, if the physical requirements for human survival are met, sexual instinct or appearance competition may also follow (Maslow 1943). After all, esteem, self-actualization and even self-transcendence may be gradually fulfilled. So far, the development of cosmetic industry is synchronized with the progress of human society that people becomes more selective and more critical on the products. On one hand, it is an unprecedented challenge for the cosmetics market. On the other hand, it is also an unparalleled opportunity for this traditional industry that comes along with the progress of human civilizations (Laval 2011).

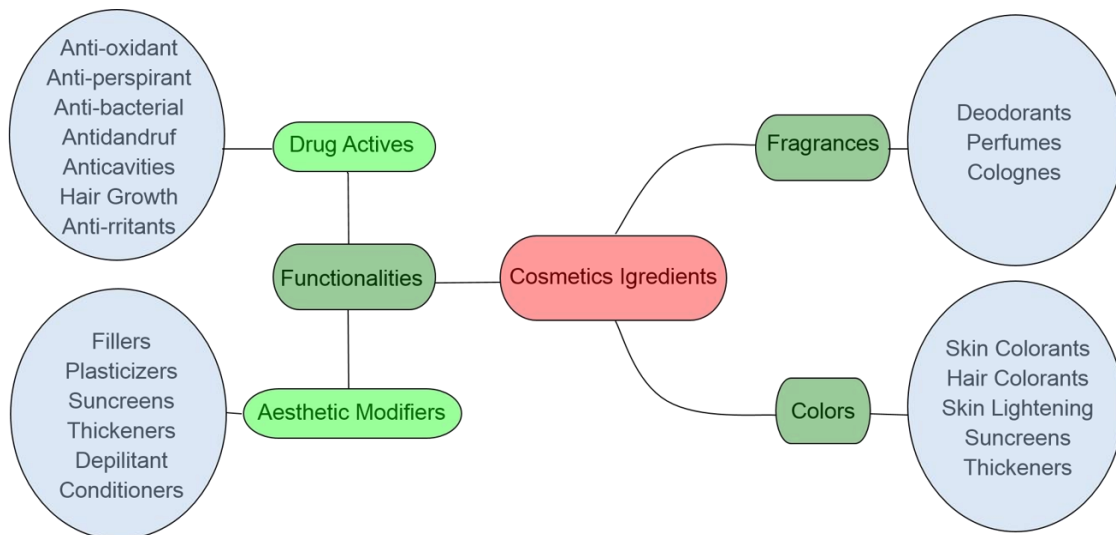


**Figure 1.1** General ingredients of cosmetics (Kumar 2005)

## **1.2 Background information on water pollution**

### **1.2.1 Heavy metal pollution**

Heavy metal pollution is more common than the public thinks because many people believe that it is only associated with areas of intensive heavy industry. However, transportation is one of the largest resources for heavy metal pollution (Forman and Alexander 1998). The large scale of fuel combustions and the growing extent of road buildings contributed significantly to the release of heavy metals, such as copper, zinc and lead (Forman and Alexander 1998). After the banning of leaded gasoline, copper and zinc became the most common heavy metals discharged from automobiles, accounting for more than 90% emission of the total metals in the road runoff (Davis, et al. 2001). The solubility and stability allow those heavy metals to readily enter aquatic systems. Once aquatic systems were contaminated by these toxic metal ions, organisms are easily to be affected through the fast mass transfer process. Even a short-term and low-level exposure to such contaminated environment will induce irreversible health effects, including acute renal failure, brain damage and immunologic disorders (Plum, et al. 2010). Additionally, heavy metals are classified as human carcinogens according to the reports by the U.S Environmental Protection Agency and the International Agency for Research on Cancer (Tchounwou, et al. 2012). High toxicity, non-biodegradability and cumulative effects of heavy metals resulted in a series of problems in living systems that the geochemical cycles and biochemical balances will be altered (Dallinger, et al. 1987). Eventually, all creatures in the food chain will be affected (Peralta-Videa, et al. 2009). To halt or reverse the

degenerating course of biological variability and sustainability in the entire ecosystem, substantial actions must be taken immediately to control the discharge of heavy metals and other poisonous compounds.

<b>Heavy Metal</b>	<b>Effect on Human Health</b>	<b>MCL (mg/L)</b>
Ar	skin manifestations, visceral cancers, vascular disease	0.05
Cd	renal dysfunction, lung cancer, bronchitis, bone defect	0.01
Cr	nervous system damage, nausea, vomiting	0.05
Cu	liver damage, stomach irritation, Wilson disease	0.25
Ni	chronic asthma, coughing, human carcinogen	0.20
Ze	corrosive effect on skin, lethargy	0.80
Pb	mental retardation and gastrointestinal damage	0.06
Hg	spontaneous abortion, rheumatoid arthritis	0.0003

**Table 1.1** The effects of heavy metals & Maximum Contaminant Level (Fu, et al. 2011)

### 1.2.2 Other pollution sources

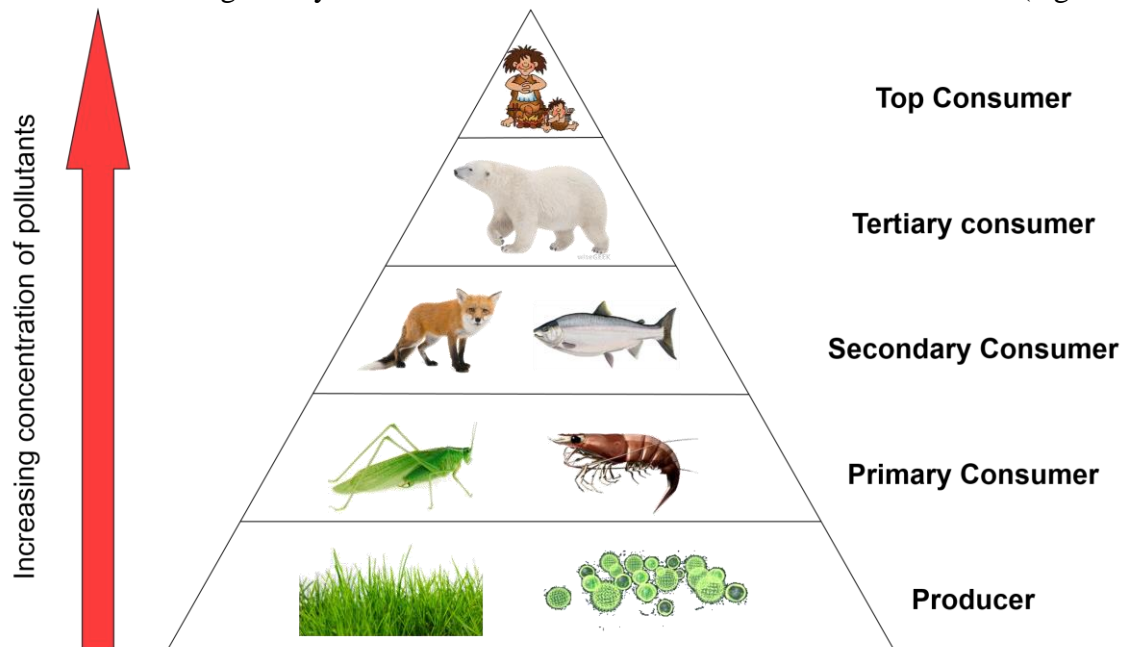
Besides heavy metal pollution, many different types of organic chemicals can cause severe problems when the tolerance exceeded (Bailey, et al. 1999). The most common and undesirable source of organic chemicals is the family of synthetic dyes. They have been used extensively in textile, pharmaceutical, packaging, cosmetics and paper industry. According to an estimation, more than  $5 \times 10^5$  tons of organic dyes are produced annually while up to  $2 \times 10^5$  tons of those dyes are lost every year to effluents due to the inefficiency in operations and the emission under no regulation (Chequer, et al. 2013). In terms of the quantity and volume, azo dyes that contain -N=N- are the largest class in industries (Van

der Zee and Villaverde 2005). Similar to heavy metals, a certain number of azo dyes are also extremely stable and they are persistent to temperature and light. Likewise, they are highly toxic that irreversible health effects on human body can be generated (McMullan, et al. 2001). Those undesirable features arise a series of difficult tasks in the treatment of effluents from synthetic dyes related industries. How to address these environmental unfriendly problems is of relevance to the future health of mankind. On one hand, industrial process is an irreplaceable part in the advancement of human civilizations. On the other hand, the eco-environment, as the key to the future, cannot be sacrificed in the name of economic growth.

### **1.2.3 Pollution control methods**

A number of novel technologies, spanning from coagulation/flocculation, electro-dialysis, chemical precipitation, ion-exchange and adsorption, have been developed over the last decade (Fu, et al. 2011). Although all methods have proved their capacity to remove heavy metal ions and dye molecules from aqueous system, they still possess some inherent disadvantages and limitations. For example, complexing agents will hinder the precipitation process and the precipitation are known as a significant producer of sludge (Kongsricharoern and Polprasert 1995). Ion exchange has been widely used to remove metal ions due to their fast kinetic and high capacity. However, it still faces the challenges from secondary pollution, which is the resin regeneration process (Kongsricharoern and Polprasert 1995). Coagulation/flocculation has received considerable attentions due to their dewatering characteristics and improved sludge settling, but a large amount of chemical

agents are consumed to form stable gelatinous mass (Kurniawan, et al. 2006). Meanwhile, fouling/scaling, low permeate flux and high press drop are frequent difficulties for membrane filtration (Blöcher, et al. 2003). Adsorption, as a full-fledged method to remove pollutants from waste water, offers flexibility in the process design as well as produces high-quality treated effluent. In most cases, adsorption based technology can remove heavy metal ions and organic dyes with less fluctuations in different of circumstances (Ngah and



Hanafiah 2008).

**Figure 1.2** The accumulation of pollutants in the food chains

### **1.3 Research scope**

The research described in this thesis is concentrated on two main topics:

#### **(a) The preparation of poly(2-hydroxyethyl methacrylate)-cellulose nanocrystals grafted fullerene (pHEMA-CNC-g-C<sub>60</sub>)**

First, the structure of pHEMA-CNC-g-C<sub>60</sub> and the grafting degree of fullerene were investigated. Secondly, the proposed reaction mechanism between fullerene and pHEMA-CNC was confirmed. Lastly, the anti-oxidant property was evaluated, involving the scavenging of a typical stable free radicals, 2,2-diphenyl-1-picrylhydrazyl (DPPH), in ethanol/water system. Based on the 1<sup>st</sup> order modeled pseudo reaction, the rate constant was obtained and the anti-oxidant performance can be quantized.

#### **(b) The preparation of poly-dopamine CNF aerogels**

The optimized CNF aerogels were used to remove copper ions and methyl orange from the aqueous phase. First, the optimal conditions to form aerogels were discussed. Secondly, the coating and cross-linking process was confirmed by FTIR. In the adsorption studies, copper(II) ions and methyl orange were chosen as the adsorbates. The kinetic study was investigated using a pseudo 2<sup>nd</sup> order model and intra-particle diffusion model. The equilibrium adsorption characteristics for the optimized adsorbent formulation were modeled using the Langmuir adsorption isotherm. The parameters associated with the adsorption process were also determined. Lastly, the effects of solution pH were also investigated to achieve an optimal adsorption conditions.

## **1.4 Thesis outline**

This thesis consists of 6 chapters. Chapter 1 provides the background information, current problems and research motivations, as well as the research scopes. Chapter 2 provides an insightful and detailed literature review describing some of current studies, involving carbon based materials and natural polysaccharide in applications. Special attentions are paid to the soluble fullerene and fullerene derivatives. Meanwhile, the potential of CNF based foam/aerogel is discussed as well. Chapter 3 addresses the first theme listed in the research scope and is titled, “The preparation of poly(2-hydroxyethyl methacrylate)-cellulose nanocrystals grafted fullerene (pHEMA-CNC-g-C<sub>60</sub>) and its anti-oxidant property”. Chapter 4 discusses some general theories and common mathematical models on adsorption. Chapter 5 addresses the second objective illustrated in the research scope and is titled, “Cellulose nanofibrils (CNFs) based aerogel as an adsorbent for waste water treatment”. Chapter 6 highlights general conclusions and constructive recommendations for future study.



# CHAPTER 2

Literature review

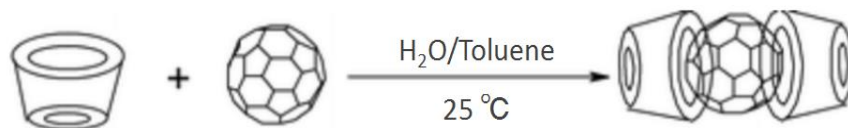
---

## 2.1 Water-soluble fullerene and its derivatives

The highly symmetric structure and the conjugated characteristics confer fullerenes a diverse range of appealing properties, such as free radical scavenging, photoluminescence and electronic conductivity (Dresselhaus, et al. 1996). However, since it was discovered, the poor solubility and the  $\pi$ - $\pi$  stacking phenomena hinder its further applications in a large scale (Bezmelnitsin, et al. 1994). Therefore, a number of methods, including hydrophilic modification, polymer graft and host-guest interaction, were used to produce water-soluble fullerene derivatives.

### 2.1.1 Host-guest interactions

In super-molecular chemistry, host-guest interaction is the design that involves more dispersed variations of electromagnetic interactions between molecules instead of creating chemical bonds (Stoddart 1988). Cyclodextrins (CDs) are the most common family of chemical compounds employed in the design of water-soluble fullerene derivatives. Typically, they are made up of sugar molecules in a ring form, also called cyclic oligosaccharides. Ranging from six to eight units, CDs with different sizes are produced respectively. Among them,  $\beta$ -CD is the most abundant and the cheapest (Wu, et al. 2001). Moreover, according to the crystallographic studies,  $\beta$ -CD owns the most suitable cavity for spherical guests (Harata 1993). As shown in Scheme 2.1, the preparation of  $\beta$ -CD/ $C_{60}$  complex with an excellent solubility was achieved by Murthy and Geckeler (Murthy and Geckeler 2001). The fullerenes embedded in this complex retained the radical scavenging activity which suggested that the surfaces of fullerenes are still accessible.



**Scheme 2.1** The synthesis of  $\beta$ -CD/C<sub>60</sub> complex (Murthy and Geckeler 2001)

In the study of Hu et al., the solubility of different host-guest systems were investigated comprehensively (Hu, et al. 1999). It turns out that the differences in solubility are not only depending on the type of CD, but also on the molar ratio between host and guest molecules. Although  $\gamma$ -CD possesses the largest cavity, the solubility of  $\gamma$ -CD/C<sub>60</sub> complex is still lower than the solubility of  $\beta$ -CD/C<sub>60</sub> complex.

System	Solubility	Highest Concentration of C <sub>60</sub> in the solution
	mg/ml	mol/L
$\alpha$ -CD/C <sub>60</sub> (1:1)	0.161	$5 \times 10^{-5}$
$\alpha$ -CD/C <sub>60</sub> (2:1)	0.468	$8 \times 10^{-5}$
$\beta$ -CD/C <sub>60</sub> (1:1)	0.643	$2 \times 10^{-4}$
$\beta$ -CD/C <sub>60</sub> (2:1)	1.713	$3 \times 10^{-4}$
$\gamma$ -CD/C <sub>60</sub> (1:1)	0.159	$5 \times 10^{-5}$
$\gamma$ -CD/C <sub>60</sub> (2:1)	0.450	$8 \times 10^{-5}$

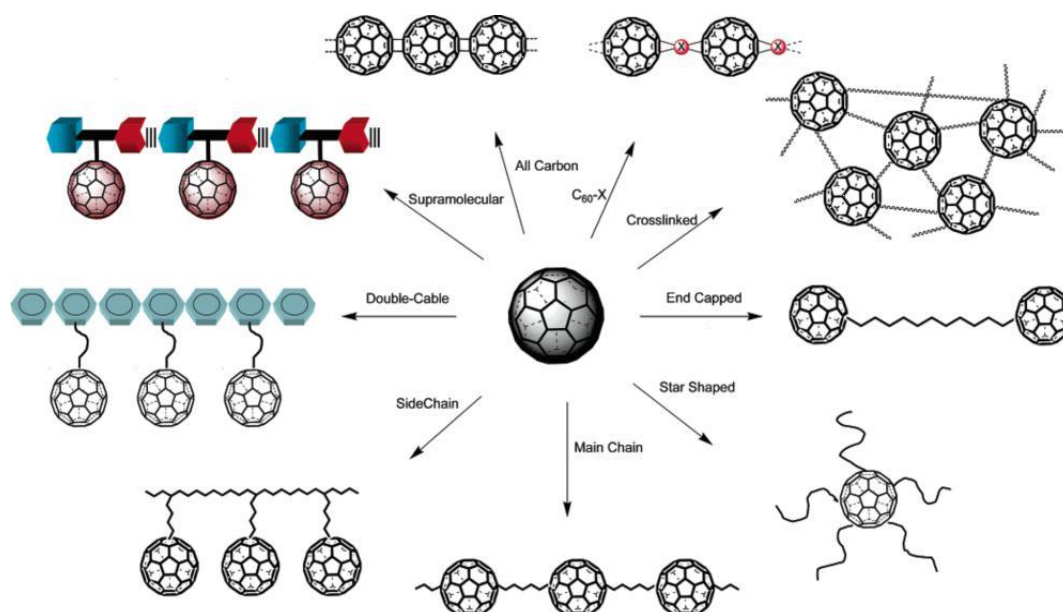
**Table 2.1** Solubility of different CD/C<sub>60</sub> complexes (Hu, et al. 1999)

### 2.1.2 Polymer-fullerene systems

The design of polymer-fullerene systems is a relatively new interdisciplinary field, where the synthesis of artificial macromolecules/supramolecules and dendrimer is applied to achieve novel functions. The patterns of fullerene based polymers, including the model

of architectures and the design of properties, are illustrated in Figure 2.1. (Giacalone and Martin 2006).

In general, there are three methods to synthesize  $C_{60}$ -containing polymers: (1) “grafting to” method: the substitutions and groups inter-changes between the target polymers and the fullerene with corresponding functionalized precursor; (2) “grafting through” method: the copolymerization of fullerene and a various kind of monomer units; (3) “grafting from” method: the employment of fullerene with functional groups and other polymers (Yao and Tam 2011).

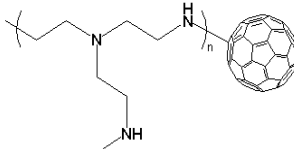
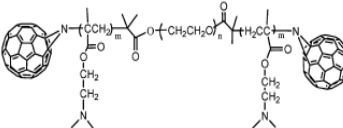
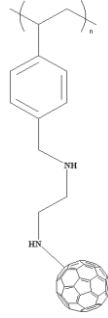
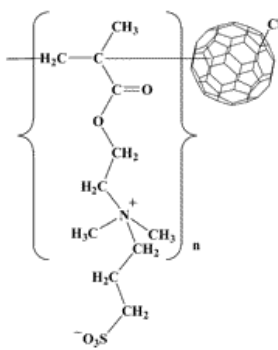
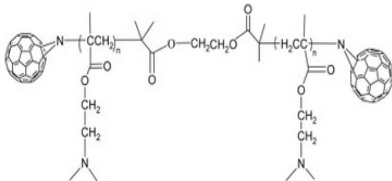


**Figure 2.1** Structures of fullerene-containing polymers (Giacalone and Martin 2006)

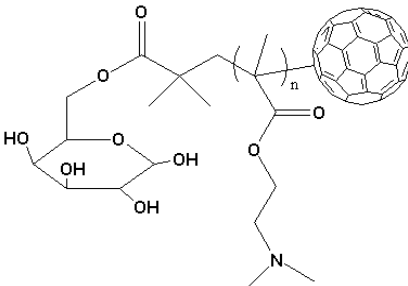
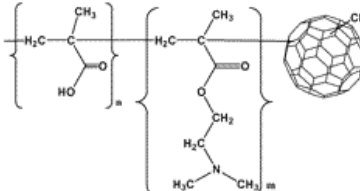
For a clear and better comprehension, the recent developed water-soluble polymer-fullerene systems are summarized in Table 2.2 (Yao and Tam 2011). A number of techniques, such as amine addition, atom-transfer radical-polymerization (ATRP), atom

transfer radical addition (ATRA) and reversible addition–fragmentation chain-transfer polymerization (RAFT) have been used to prepare C<sub>60</sub>-containing polymers.

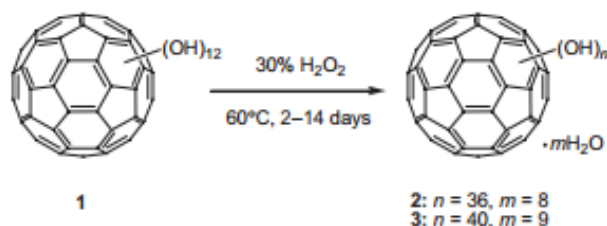
**Table 2.2** Summary of water-soluble fullerene polymeric systems (Yao and Tam 2011)

Polymers	Methods	Structures	Physical properties
<b>Poly(ethyleneimine)</b>	amine addition		solubility of C <sub>60</sub> increased
<b>PDMAEMA-b-EO-b-PDMAEMA</b>	ATRP/ azido coupling HMTETA/CuCl, NaN <sub>3</sub>		micelles formed in aqueous solution
<b>Poly[4-[(2-aminoethyl)imino]methyl]styrene</b>	amine addition		solubility of C <sub>60</sub> increased
<b>Betainized PDMAEMA-C<sub>60</sub></b>	ATRP/ATRA used 1,3-propane sultone to betainize PDMAEMA		UCST varied with salt concentration
<b>PDMAEMA-b-CH<sub>2</sub>CH<sub>2</sub>O-b-PDMAEMA</b>	ATRP/ azido coupling HMTETA/CuCl NaN <sub>3</sub>		pH - responsive self-assembly behavior

■ Table 2.2 continued.

Polymers	Methods	Structures	Physical properties
PDMAEMA with targeting moieties	ATRP/ATRA catalyzed by CuCl/HMTETA		pH-responsive self-assembly behavior
P(MAA-b-DMAEMA)	ATRP/ATRA hydrolysis to remove t-butyl group		pH/temperature responsive solubility and self-assembly behavior

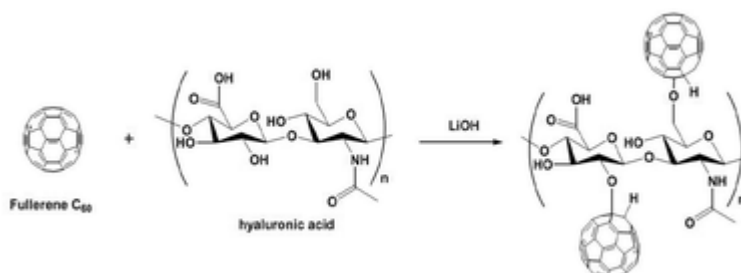
### 2.1.3 Other types of water-soluble fullerenes



**Scheme 2.2** The synthetic route of fullerol (Kokubo, et al. 2008)

Besides host-guest systems and polymeric fullerenes, water-soluble fullerene derivatives can also be obtained via hydrophilic modifications. For example, the most common water-soluble fullerene derivative, fullerol, was produced through extensive hydroxylation (Sayes, et al. 2004). Normally, it is expressed as  $\text{C}_{60}(\text{OH})_n$  with hydroxyl groups varying from 8 to 40 (Wu, et al. 2014). The number and distribution of hydroxyl

groups are dependent on synthetic routes and hydroxylation agents. To the best of our knowledge, the solubility of fullerol can approach up to 58.9 mg/ml, which is 10 orders



higher than unmodified fullerene (Kokubo, et al. 2008).

**Scheme 2.3** The synthesis of hyaluronated fullerenes (Kim, et al. 2014)

To overcome the  $\pi$ - $\pi$  stacking induced aggregation behavior, Kwag and coworkers coupled fullerenes with hyaluronic acids to prepare a novel generation of fullerene nanocomposite. The final nanomaterials are able to be dispersed in water and the photoluminescence intensity of fullerenes is preserved (Kwag, et al. 2013). Moreover, the fullerene containing nanocomposites became a kind of biocompatible and multifunctional hybrid that is applicable for tumor imaging, targeting and therapy. In a similar manner, LiOH was used to graft fullerenes onto glycol chitosan. The resulting nano-gels displayed the potential to be a candidate for endosomal pH targeting and in vivo photodynamic therapy (Kim, et al. 2014). Interestingly, the same mechanism of binding biopolymers and fullerenes was also employed between graphene nano-platelets and fullerenes. A type of carbon-based electro-catalysts for oxygen reduction reaction was produced, displaying an enhanced electro-catalytic efficiency that is much higher than pristine graphite (Guan, et al.

2015). Based on these studies, a unique perspective to treat fullerenes in aqueous phase has been brought up through the employment of nano-engineered materials and coupling agents.



## **2.2 Surface modifications of cellulose nanocrystals (CNCs)**

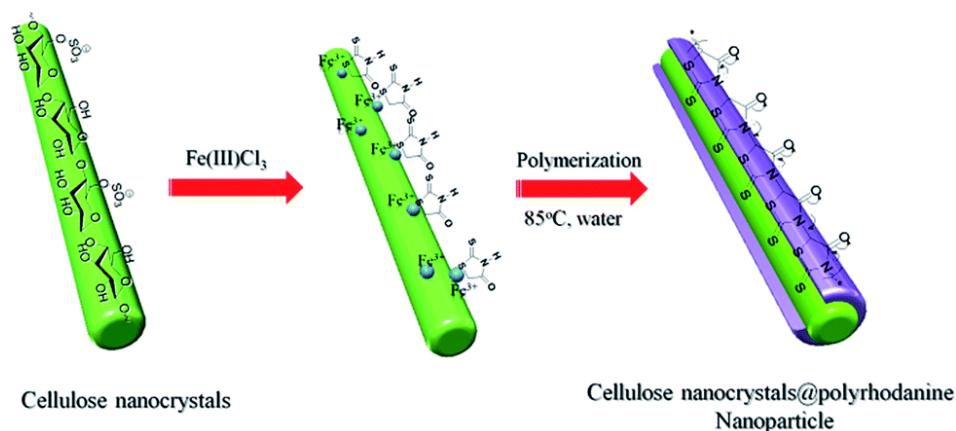
Basically, there are two common ways to modify the surface of CNCs, non-covalent modification method and covalent grafting method (Habibi, et al. 2010) (Azizi Samir, et al. 2005). The former approach is simply to use monomers or other molecules to form a layer of shell structure on the surface of CNC. Namely, there is no chemical interaction between the coating layer and the CNC. The resulting structures are formed via the weak van der Waals forces or other intermolecular forces, such as electrostatic attractions (Habibi, et al. 2010). The latter method is chemical modification through the conversion of the surface groups on CNC, or the grafting of polymers onto CNC. In detail, the chemical modification method can be categorized into two groups, the “graft from” method and the “grafting onto” method (Habibi, et al. 2010).

### **2.2.1 Non-covalent modification methods**

Non-covalent modifications are often achieved via physical adsorptions, electrostatic attractions, hydrophilic affinity, hydrogen bonds and van der Waals interactions (Siqueira, et al. 2010). Surfactants coated CNCs was the first system using this strategy to achieve well dispersed CNC suspensions in a non-polar solvent (Heux, et al. 2000). In a further study, these surfactants wrapped CNCs displayed a good compatibility when incorporating into isotactic polypropylene as nano-metric fillers (Ljungberg, et al. 2006). Some non-ionic surfactants also played important roles in this type of interaction. In the work of Rojas *et al.*, the dispersion property of the hydrophilic reinforced CNC in the hydro-phobic matrix

was improved via the non-ionic surfactant sorbitan monostearate, leading the formation of bead-free electro-spun webs (Rojas, et al. 2009).

Instead of using surfactants, some researchers used electrostatic attractions as the driving force to initiate an in-situ polymerization on the surface of CNC. Tang *et al.* introduced a facile and green approach to synthesize CNC@polyrhodanine core-shell nanoparticles as anti-microbial agents (Tang, et al. 2015). The polymerization was initiated on the negatively charged surface of CNC where the positively charged oxidants, Fe(III), was anchored via electrostatic interactions. By varying the ratio between the CNC, the monomer and the oxidant, the coating condition was optimized. This composite material also displayed a reversible color change in response to pH (Tang, et al. 2014).



**Scheme 2.4** The fabrication of CNC@polyrhodanine core-shell nanoparticles

Inspired by natural organisms, a coating strategy was developed via polydopamine. Explicitly, this polymer containing catechol groups and amine groups has a similar structure as the adhesive proteins secreted by mussels (Zhang, et al. 2013). Meanwhile, dopamine monomer itself can self-polymerize in alkaline conditions and spontaneously deposit onto larger particles. In order to immobilize and stabilize inorganic nanoparticles,

such as silver particle, CNC@polydopamine was introduced by Shi *et al.* (Shi, et al. 2015). The polydopamine-CNC is able to reduce silver ions, triggering the formation of silver nanoparticles (AgNPs) on the surface. The composite system with an improved stability performed an anti-microbial activity that is four times better than free AgNPs toward *E. coli* and *B. subtilis*.

## **2.2.2 Covalent modification methods**

### **2.2.2.1 Surface group conversion and substitution**

A series of techniques were used to convert hydroxyl groups on the surface of CNC to other functional groups, including oxidation, amidation, silylation, sulfonation, etherification and esterification (Hubbe, et al. 2008).

Most of these conversions are considered as pre-treatments prior to the eventual polymers grafting. For example, 2,2,6,6-tetramethylpiperidine-1-oxyl (TEMPO) is often used to facilitate the disintegration process by breaking the strong hydrogen bonds in cellulose. This TEMPO-mediated oxidation is a highly selective reaction, where only primary hydroxyl groups are converted into carboxyl groups (De Nooy, et al. 1994). After treatment of TEMPO, the oxidized surface became negatively charged and the stability of CNC suspensions in water is improved due to the induced electrostatic repulsions (Araki, et al. 2000).

Another reputable technique for surface modifications is proposed by Fischer and Speier, which is known as Fischer esterification (Fischer and Speier 1924). It has been reported that the simultaneous hydrolysis of amorphous cellulose triggered by the Fisher

esterification caused the isolation of acetylated CNCs through a one-pot reaction (Braun and Dorgan 2008). Furthermore, an environmentally friendly route to realize the surface acetylation was proposed by Yuan and co-workers (Yuan, et al. 2006). In their study, alkenyl succinic anhydride (ASA) aqueous emulsions were employed as templates to mix with CNC suspension, leading to the formation of hydrophobic domains.

In most cases, the purpose of surface group substitution is to enhance the stability for CNC suspensions in different solvents, like water or DMSO. These pre-treatments laid the basis for further functionalization.

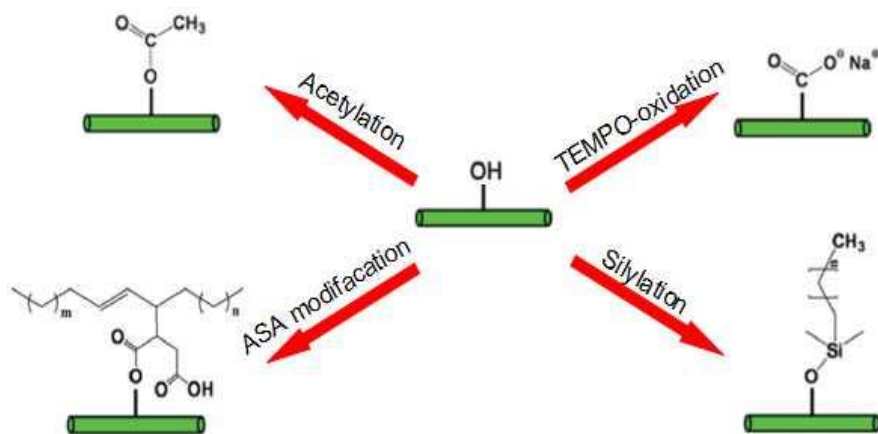
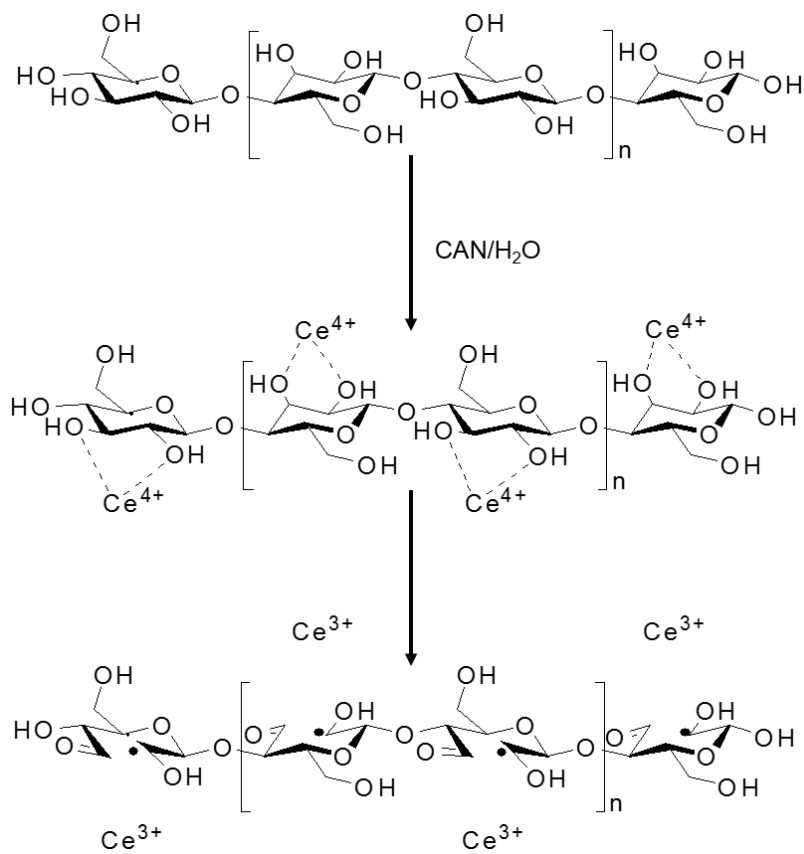


**Figure 2.2** Surface conversion and substitution of CNC (Lin, et al. 2012)

### 2.2.2.2 The “graft from” method

In the “graft from” method, polymer chains grow from the initiating sites on the cellulose surface or backbone. This strategy was first reported by Habibi *et al.*, who used stannous octoate ( $\text{Sn}(\text{Oct})_2$ ) as initiators to successfully graft polycaprolactone onto CNC (Habibi, et al. 2008). Recently, cerium (IV) ammonium nitrate (CAN), as a free radical producer and polymerization initiator has generated a great deal of attention due to its

ability to cleave the monosaccharide units (Kan, et al. 2013). A wide range of polysaccharide polymeric composites were fabricated using this initiator, such as poly(2-hydroxyethyl methacrylate)-g-kappa-carrageenan (Sadeghi and Hosseinzadeh 2010), poly(4-vinylpyridine)-g-CNC (Kan, et al. 2013), poly(methyl acrylate)-g-starch (Rahman, et al. 2000) and polyacrylonitrile-g-chitosan (Pourjavadi, et al. 2003). The mechanism of radical production by using CAN is illustrated in Scheme 2.4.



**Scheme 2.4** The mechanism of CAN to activate cellulose

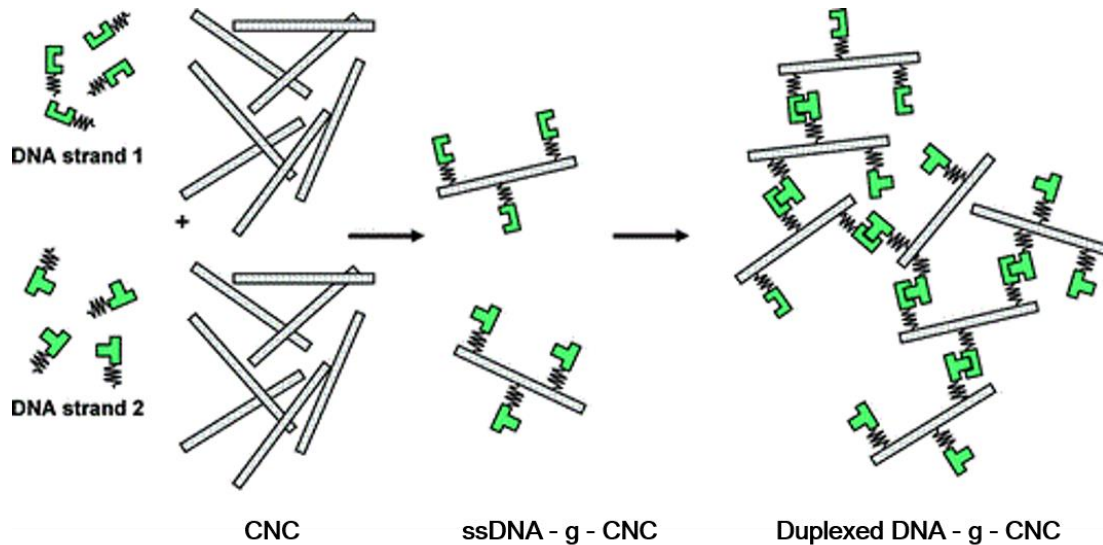
In the case of CNC, there is also a number of polymers that have been effectively grafted by using this initiator, such as poly(acrylamide-methylacrylate) (Gupta and Khandekar 2002), poly(acrylonitrile-ethylmethacrylate) (Gupta and Sahoo 2001), poly(N-isopropylacrylamide) (Gupta and Khandekar 2003), poly(acrylamide-methylmethacrylate) (Gupta and Khandekar 2003) and polyacrylamide (Gupta and Khandekar 2006). With the assistance of these polymers, a wide range of functionalities can be transferred into CNC composite systems, such as thermos-responsive behavior, pH-responsive behavior, self-assembly and photo-responsive behavior.

### **2.2.2.3 The “graft onto” method**

In the “graft onto” method, pre-synthesized polymer chains were coupled onto the surface of CNCs via coupling agents. The most significant advantage of this strategy is that it allows researchers to fully characterize the target polymers as well as tuning their properties (Lin, et al. 2012). However, this approach is like a double-edged sword that comes with unfavorable consequences. For example, the polymer grafting degree is inherently hindered due to the steric effects, especially when the pre-synthesized polymers are in the form of branches or dendrimers (Kalashnikova, et al. 2013).

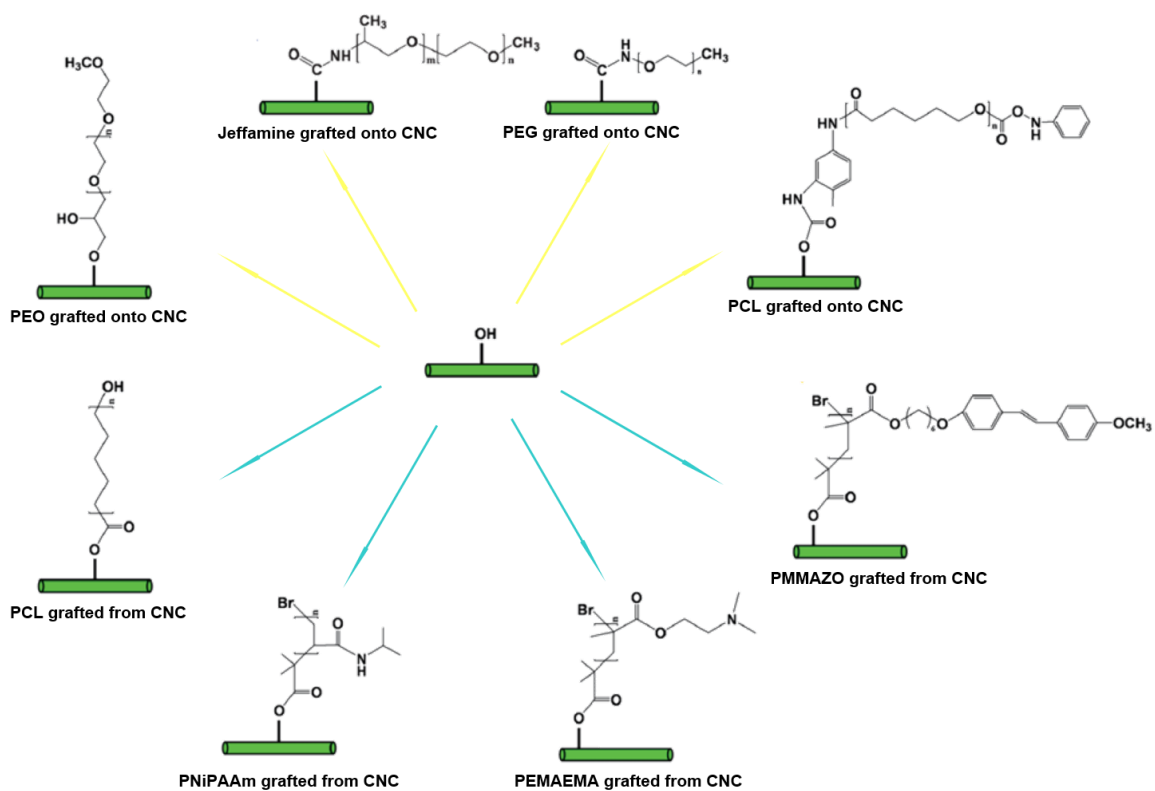
In spite of these limitations, this technique was still successfully used to graft a number of polymers onto CNC. For example, Ljungberg *et al.* prepared nanocomposite films by incorporating CNC with maleated polypropylene (Ljungberg, et al. 2005). A high dispersion level and a good compatibility in atactic polypropylene were obtained. In the work of Mangalam *et al.*, two different kinds of amino-modified ss-DNAs were grafted

onto TEMPO-oxidized CNCs via dehydration condensation (Mangalam, et al. 2009). The resulting nanocomposites showed a reversible hybridizing property due to the presence of duplexed DNA.



**Scheme 2.5** The design of duplexed DNA-g-CNC (Mangalam, et al. 2009)

In conclusion, surface modification and polymer grafting expanded the applications of CNC. Tools to tailor CNC based systems are available now due a wide variety of techniques and materials. Especially with the advancement of nanotechnology, experimental designs inspired by innovative ideas have emerged. Not only the microstructures of CNC based systems can be precisely controlled, both chemical and physical properties can be accurately managed as well. Admittedly, this cellulose nano-material is still in its infancy, but revolutionary milestones and advancing breakthrough are anticipated (Duran, et al. 2011).



**Scheme 2.6** Common polymers used in chemical grafting method (Lin, et al. 2012)



# CHAPTER 3

The preparation of poly(2-hydroxyethyl methacrylate)-cellulose nanocrystals grafted fullerene (pHEMA-CNC-g-C<sub>60</sub>) and its anti-oxidant property

---

### 3.1 Introduction

Fullerene, a well-known allotrope of carbon, is one kind of extremely symmetric molecule in the shape of hollow sphere. It was first discovered by Kroto and Heath in 1985, which was presented as a highly stable cluster that contained 60 carbon atoms (Kroto, et al. 1985). They suggested a truncated icosahedron structure for this bulky-ball species, consisting of 12 pentagons and 20 hexagons. In 1990, the successful manufacture of fullerene in gram-scale marked the beginning of a new era of carbon-based materials (Kr äschmer, et al. 1990). Since then, a considerable amount of attention has been paid to fullerenes due to their enormous and untapped potentials in the realm of electrochemistry (Thompson and Frechet 2008), bio-medicine (Markovic and Trajkovic 2008), photodynamic therapy (Imahori and Sakata 1997), solar energy (Xiong, et al. 2012) and other applications (Partha and Conyers 2009). Notably, advancements in nano-engineering and nano-technology afford modern scientists with an insightful view on the research of fullerenes.

However, one critical imperfection that limits the applications of fullerenes is its extremely low solubility in water. In another words, fullerenes are not water-processable due to the intrinsic hydrophobicity and the  $\pi$ - $\pi$  stacking induced aggregation. Therefore, several methods were applied to synthesize water-soluble fullerene derivatives. Among them, the most common method is to graft highly hydrophilic polymeric chains onto fullerenes. For example, a water-soluble fullerene derivative was prepared by the cycloaddition reaction between monoazido-terminated poly(ethylene oxide) and C<sub>60</sub>

(Huang and Goh 2000). Attractively, Dai et al. reported a self-assembly behavior of water-soluble fullerene-containing poly[2-(dimethylamino)-ethyl methacrylate] (PMMA) (Dai, et al. 2004). Another popular approach to obtain water-soluble fullerene is surface modification. For example, a class of highly hydroxylated fullerenes, also called fullerol, was produced through hydroxylation, where the solubility was enhanced by the extensive introduction of hydroxyl groups. Moreover, the host-guest complex that encompasses the design of molecular interactions and complementarities via non-covalent forces offers an extra option to solubilize fullerene, such as embedding them into cyclodextrins (Samal and Geckeler 2000) (Yao and Tam 2014).

To overcome some drawbacks of fullerenes, such as the insolubility and the  $\pi$ - $\pi$  stacking induced aggregation behavior, a nano-sized polysaccharide material - cellulose nanocrystals (CNCs) - was introduced. CNC is a type of cellulose based nano-material with an exceedingly large surface area. It is one of the most sustainable and renewable building blocks in the biosphere. Besides, the large annual yield of cellulose, assessed to be more than  $7.5 \times 10^{10}$  tons, makes it one of most abundant biomass material (Habibi, et al. 2010). In general, it is the attainability, biodegradability, biocompatibility, smooth processability, excellent mechanical strength and large-reactive surface area that contributed to the major advantage of CNC over other natural polymeric structures (Habibi, et al. 2010). Hence, a significant attention has been paid to this structural building block, where chemical-physical modifications and treatments were incorporated into CNC based systems.

In this chapter, we report an approach of combining fullerenes with CNCs, producing

an anti-aging product with an excellent stability in water. In addition to the production of water-processable fullerenes, the large-reactive surface area of CNC affords enough anchoring sites for the conjugation of functionalities to yield an excellent radical-scavenging compound. This novel generation of fullerene/bio-nanomaterial derivatives enriched the methods of tailoring nano-composite materials and extended the scope of applications. Therefore, this combination provided a long-term vision for the future progress of nanotechnology, in particular within the realm of CNC.

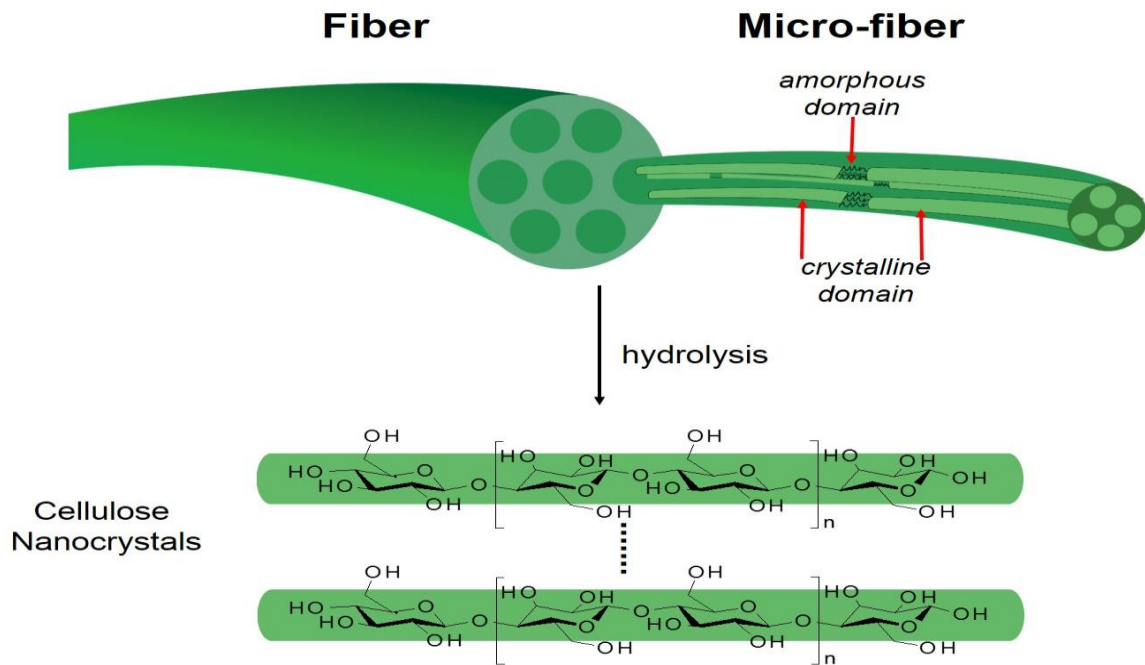


**Figure 3.1** The morphology of cellulose nanocrystals

## **3.2 Experimental section**

### **3.2.1 Materials**

Cellulose nanocrystal (CNC) were provided by CelluForce (Winsor, QC, Canada) with an average surface area of 500 m<sup>2</sup>/g. 2-hydroxyethyl methacrylate (HEMA), ammonium cerium (IV) nitrate (CAN), lithium hydroxide (LiOH), toluene and dimethyl sulfoxide (DMSO) were purchased from Sigma-Aldrich. Fullerene were acquired from MTR, Ltd (Cleveland, OH, U.S). In the test of anti-oxidant property, 2,2-diphenyl-1-picrylhydrazyl (DPPH) and reagent alcohol (EtOH) were obtained from Sigma-Aldrich and Fisher-Scientific, respectively. All chemicals and solvents were used without further purification.

### **3.2.2 Methods**

#### **3.2.2.1 Synthesis of pHEMA-CNC**

At first, 2.0 g CNC was dispersed in 400 ml Milli-Q water using an IKA homogenizer to produce a transparent dispersion. Then, 1.0 g of HEMA monomers was added to the CNC-dispersion, followed by a vigorous stirring and degassing. After mixing and N<sub>2</sub>-bubbling, 80 mg of CAN was introduced to the aqueous system to initiate the polymerization. The reaction was conducted under vigorous stirring overnight at 45 °C, and the purified pHEMA-CNC sample was obtained through centrifugation.

#### **3.2.2.2 Synthesis of pHEMA-CNC-g-C<sub>60</sub>**

In the second reaction vessel, 20 mg of pre-prepared pHEMA-CNC was transferred into 20 ml DMSO by solvent exchange. Then, a C<sub>60</sub>-toluene solution (30 mg in 10 ml) was

mixed with CNC/DMSO. After 30 mins of vigorous stirring, 6 mg LiOH was added to the homogeneous system to initiate the conjugation reaction. Then, the reaction was maintained at room temperature for the next 5 days with vigorous stirring. Afterwards, vacuum oven was used to remove the solution (dark-brown/black color) was transferred to a dialysis tube for a 5-day dialysis (water was replaced every 4 h). Finally, the freeze-dried pHEMA-CNC-g-C<sub>60</sub> sample was obtained (brown color). All steps in the second process were conducted under dim light or no light.

### **3.2.2.3 The protocol of anti-oxidant test**

The protocol of assessing the free radical scavenging was adopted from Geckeler and Bondet with a few modifications (Geckeler and Samal 2001) (Bondet 1997). The specific procedures are described as follow.

#### **1. The Preparation of Solutions:**

The pHEMA-CNC-g-C<sub>60</sub> aqueous solution was prepared by dissolving 5mg pHEMA-CNC-g-C<sub>60</sub> sample into 5mL Milli-Q water, which underwent a series of dilutions to yield a 0.25 mg/ml solution. DPPH was dissolved in EtOH that resulted in a stable free radical solution with a purple color (0.002 mg/ml). Noticeably, DPPH/EtOH solution was always freshly prepared.

#### **2. UV-vis Scanning:**

First, well-mixed H<sub>2</sub>O/EtOH solution (volume ration 1:1) was used to calibrate the UV-vis spectrometer. After calibration, 1 ml of anti-oxidant solution and 1 ml of DPPH solution

were successively added to the cleaned cuvette. Pipette and cuvette stir bar were used to accelerate the mixing process. Before the UV-vis scanning, cuvette caps were used to seal both cuvettes. As the pre-scheduled measuring configuration, the reaction was scanned for 200 mins (every 5 mins for the first 100 mins and every 10 mins for the rest 100 mins) to obtain the time dependent absorption curves.

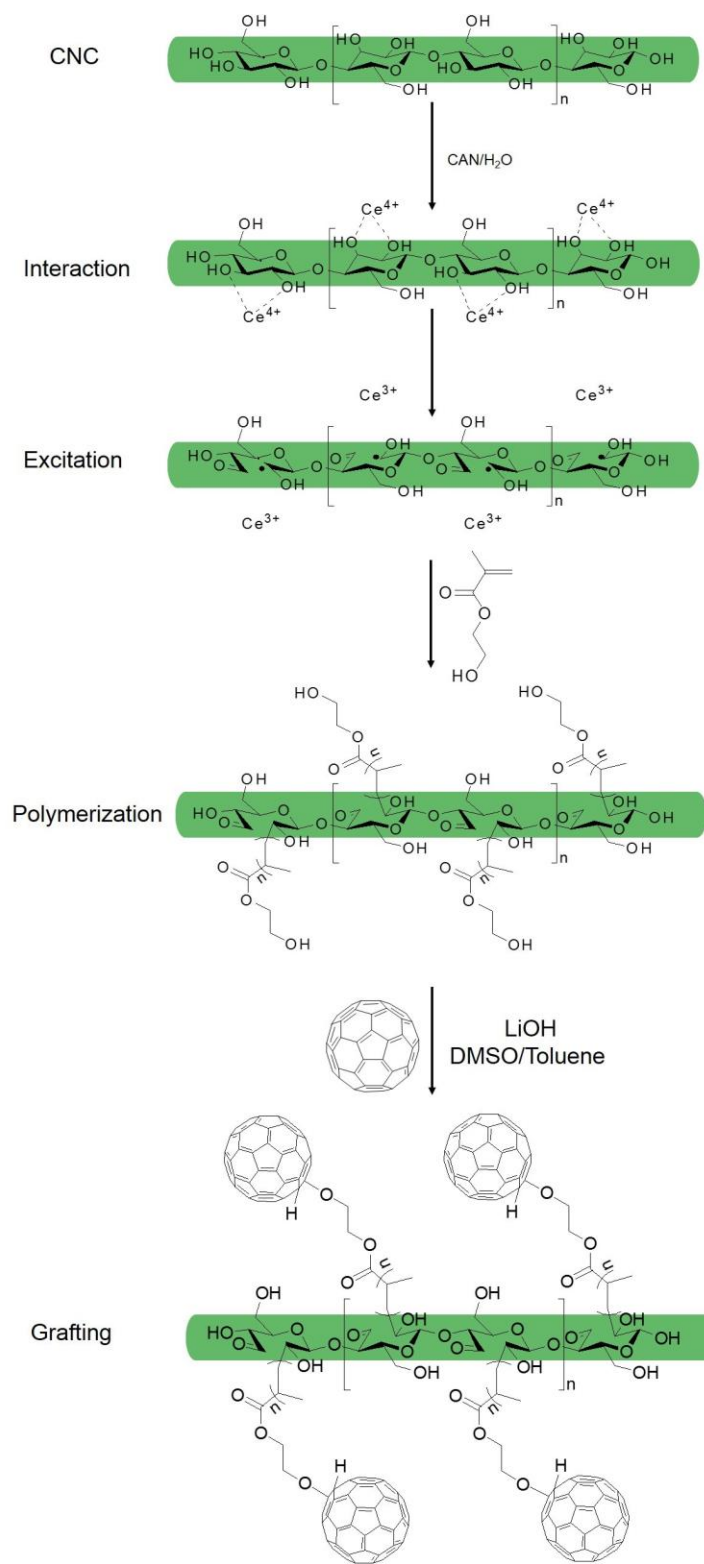
### 3.3 Characterizations

#### 3.3.1 The mechanisms of synthesis

The pHEMA-CNC-g-C<sub>60</sub> was fabricated through a two-pot synthesis. At first, the “graft from” strategy was employed with the assistance of CAN. As the initiator, CAN is able to open repeating saccharide units in CNCs and produce free radicals on the surface of CNC (Gupta and Khandekar 2002). The activated surface sites on CNC will play a role as anchor points during the formation of polymer chains.

After polymer grafting, the second step was processed to conjugate fullerenes onto CNC and polymer brushes. In this stage, LiOH was added to the miscible reaction system to facilitate the conjugating reaction between pHEMA-CNC and fullerene (Kwag, et al. 2013). The mechanism behind this reaction is that LiOH is able to pre-activate the  $\pi$ - $\pi$  carbon bonds, yielding activated fullerenes (Guan, et al. 2015). Then, reactive hydroxyl groups can conjugate with fullerenes via carbon-oxygen covalent bonds. The schematic procedures of overall synthesis are illustrated in Scheme 3.1.





**Scheme 3.1** The overall process to synthesize pHEMA-CNC-g-C<sub>60</sub>

### 3.3.2 Fourier Transformation Infrared Spectroscopy (FT-IR)

Figure 3.2 showed the FT-IR spectra of pristine CNC, pHEMA-CNC and pHEMA-CNC-g-C<sub>60</sub>, all of which confirmed the existence of pHEMA and fullerene. The peaks appearing around 1725 cm<sup>-1</sup> and 1451 cm<sup>-1</sup> in the blue curve can be attributed to the stretching vibration of C=O groups and bending vibration of C-H bonds, respectively (Dahman 2012) (Zhao, Zhang, et al. 2012) (Mansur, et al. 2008). The presence of pHEMA was confirmed by the two characteristic peaks (Belfer, et al. 2004) (Singh and Ray 1994) (Zheng and Stöver 2002). Furthermore, the evident peaks near 527 cm<sup>-1</sup>, 575 cm<sup>-1</sup>, 1180 cm<sup>-1</sup> and 1429 cm<sup>-1</sup> in the green curve are the characteristic peaks of fullerene (Haufler, et al. 1990) (Guan, et al. 2015) (Jeong, et al. 2012). Hence, the FT-IR spectra verified that the final product with brownish color possessed pHEMA and fullerenes.

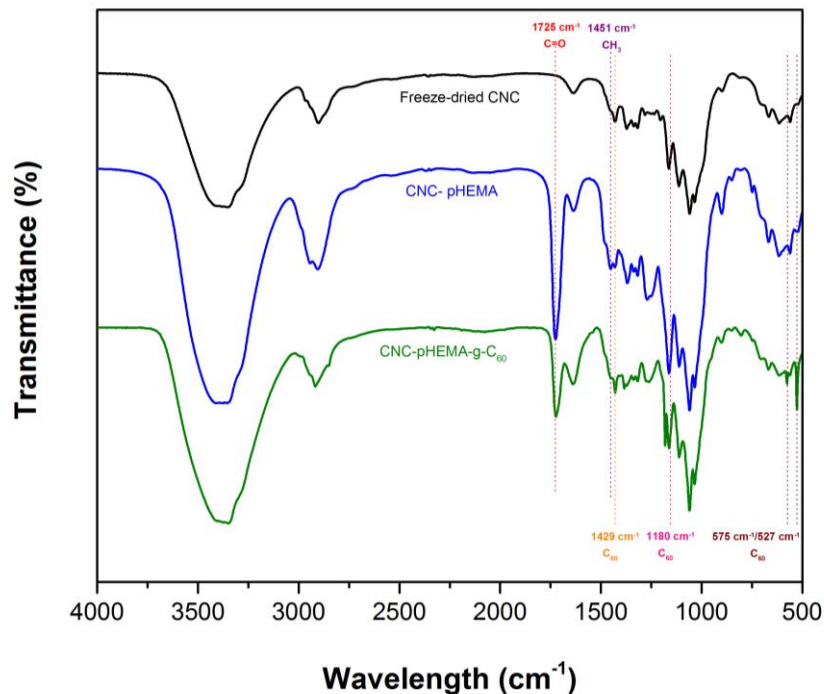


**Figure 3.2** FTIR spectra of CNC, pHEMA-CNC and pHEMA-CNC-g-C<sub>60</sub>

### 3.3.3 Proton Nuclear Magnetic Resonance ( $^1\text{H-NMR}$ )

To verify the proposed mechanism of conjugation depicted in Figure 3.2,  $^1\text{H-NMR}$  was used. The spectrum in Figure 3.3 can be used to analyze the structure of pHEMA-CNC-g- $\text{C}_{60}$ . Firstly, the peak at 6.5ppm (-CH on fullerene units) was a substantial evidence that supports the conjugating reaction between fullerene and -OH groups (Kwag, et al. 2013) (Kim, et al. 2014). This peak indicated that fullerenes were covalently immobilized onto pHEMA-CNC, resulting in chemically stable products. Hence, the introduction of LiOH to catalyze the reaction has been validated (Bontempo, et al. 2004) (Kong, et al. 2004). The corresponding groups of other peaks are exhibited in Figure 3.3.

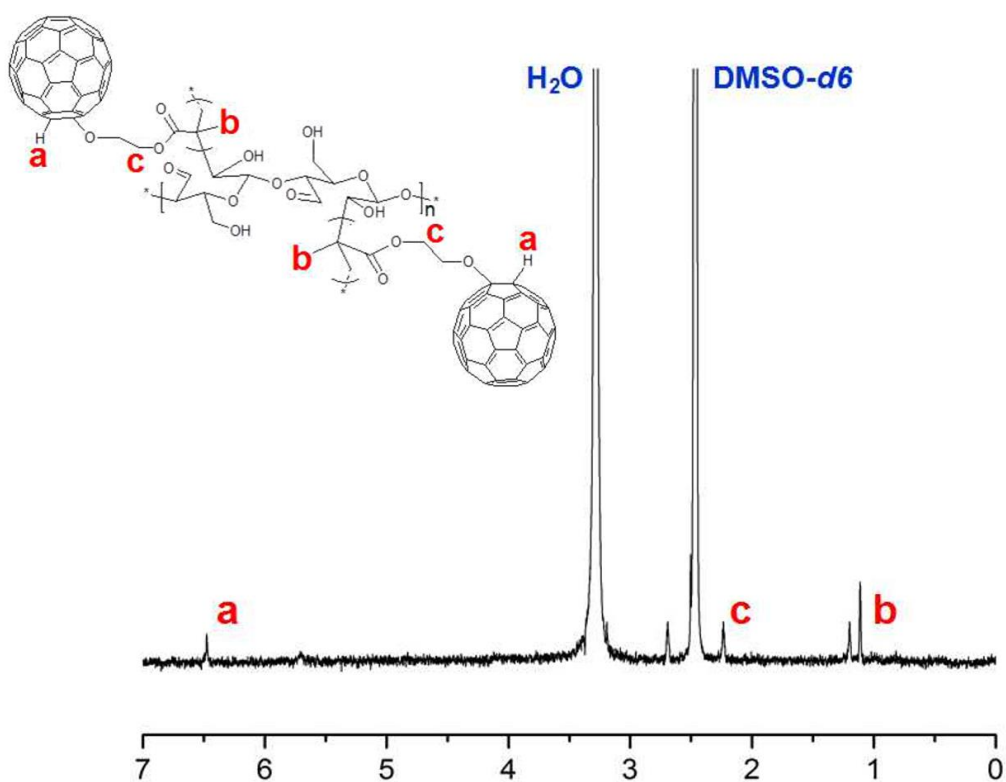


**Figure 3.3**  $^1\text{H-NMR}$  spectrum of pHEMA-CNC-g- $\text{C}_{60}$



### 3.3.4 Thermal Gravimetric Analysis (TGA)

TGA was used to further estimate the grafting degree of fullerenes onto pHEMA-CNC. Firstly, no weight loss was observed from the curve of pristine fullerene during the continuous heating period, indicating an excellent thermal stability of fullerene. As for pHEMA-CNC, this cellulose based material started decomposing around 190 °C. By comparing the TGA residues between pHEMA-CNC and pHEMA-CNC-g-C<sub>60</sub>, the grafting degree of fullerene onto pHEMA-CNC was estimated to be 46.3%. This grafting degree evidently reflected the highly catalytic activity of LiOH in the coupling reaction between fullerenes and pHEMA-CNC.

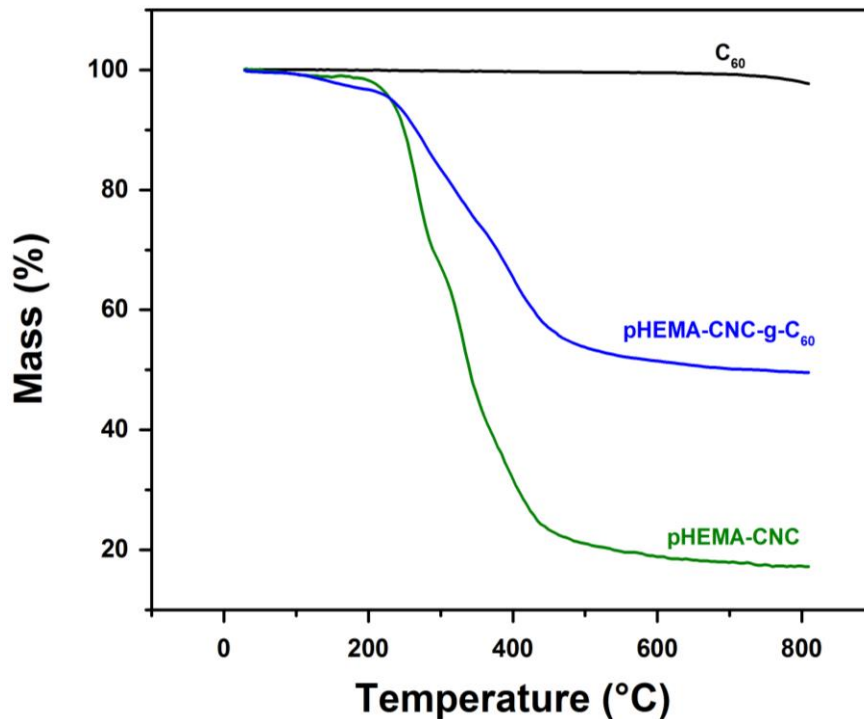


**Figure 3.4** TGA profile of C<sub>60</sub>, pHEMA-CNC and pHEMA-CNC-g-C<sub>60</sub>

### 3.3.5 The anti-oxidant property

The anti-oxidant behavior was investigated by the UV-vis scanning for 200 min as shown in Figure 3.5. Both fullerene composites and water showed the ability to reduce the concentration of DPPH.

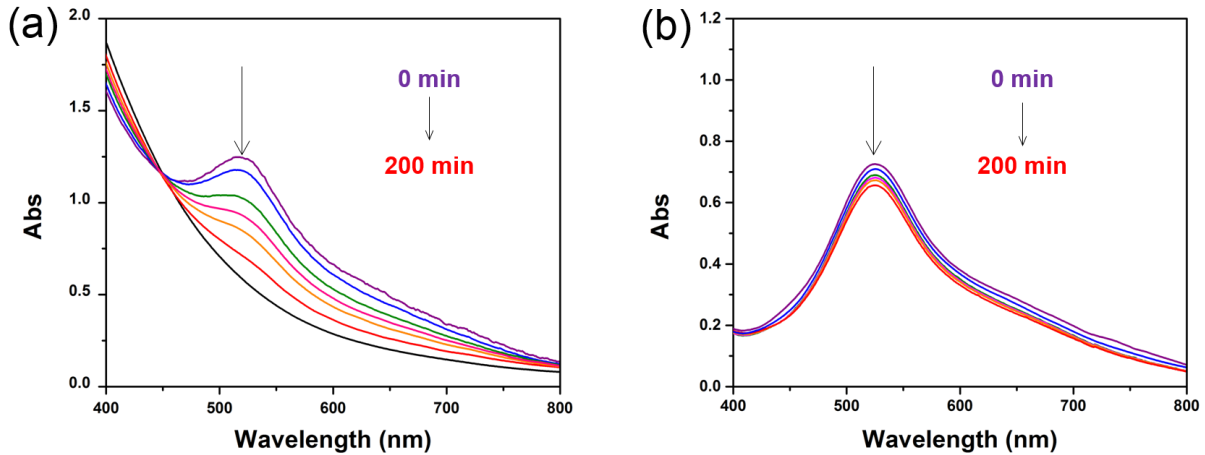


**Figure 3.5** Time dependent UV-vis spectra for the oxidation of DPPH

(a) pHEMA-CNC-g-C<sub>60</sub> vs DPPH; (b) H<sub>2</sub>O vs DPPH;

In the test of anti-oxidant performance, the concentration of fullerene particles was rather challenging to be continually measured via UV-vis spectrophotometry, thus a pseudo 1<sup>st</sup> reaction was assumed (Sin, et al. 2005). By doing this, the anti-oxidant property can be quantified.

---

2<sup>nd</sup> order reaction:

$$rate = k \cdot [A] \cdot [B]$$

assumption:  $k' = (k \cdot [A])$

$$rate = (k \cdot [A]) \cdot [B]$$

pseudo 1<sup>st</sup> order reaction:

$$rate = k' \cdot [B]$$


---

$k$  : the constant in the 2<sup>nd</sup> order reaction

$[A]$  : the concentration of compound A

$[B]$  : the concentration of compound B

$k'$ : the constant in the pseudo 1<sup>st</sup> order reaction

---

In order to fit in pseudo 1<sup>st</sup> reaction, the concentration of DPPH needs to be manipulated to a significantly low level while the concentration of pHEMA-CNC-g-C<sub>60</sub> is relatively high. During the reaction, the concentration of DPPH decreased gradually while the quantity variation of fullerenes was almost negligible (Geckeler and Samal 2001). After several trials, 0.002 mg/ml and 0.25 mg/ml were found to be the desirable initial concentrations for DPPH and pHEMA-CNC-g-C<sub>60</sub>, respectively. Equation 3.1 was used to calculate the rate constant, which intuitively defines the quantitative basis of this free radical scavenging reaction (Tam, et al. 2013).

$$-k \cdot t = \ln \frac{A_{\infty} - A_t}{A_{\infty} - A_0} \quad (3.1)$$

$t$ : the reaction time (min)

$A_t$ : the absorbance at time  $t$

$A_0$ : the absorbance at initial

$A_{\infty}$ : the absorbance at time infinity (one week after the test)

$k$ : the reaction rate (min<sup>-1</sup>)

As shown in Figure 3.6, the kinetic curve displays a linear regression over the entire period of free radical scavenging after eliminating the impacts of water. The reaction rate was calculated to be 0.008 min<sup>-1</sup>.

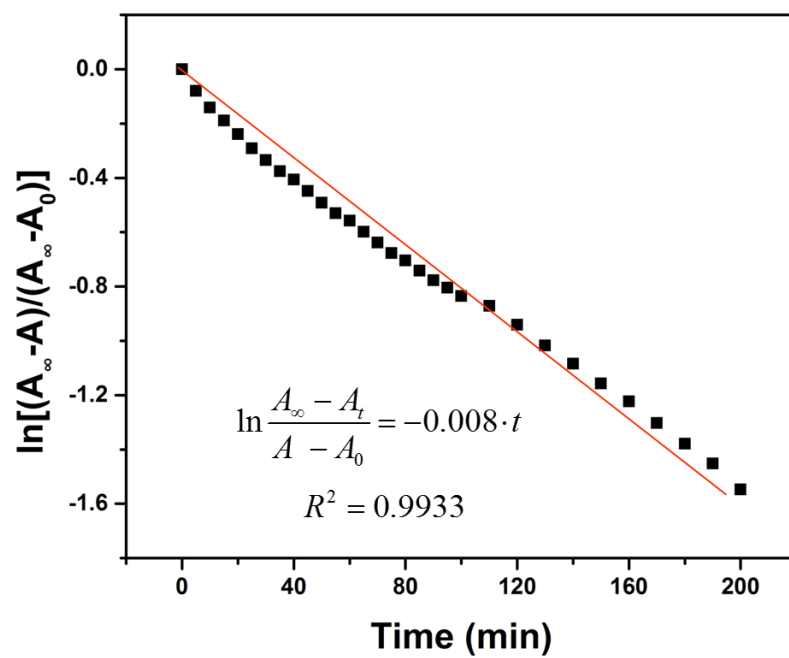


**Figure 3.6** The kinetic curve of free radical scavenging



### 3.4 Conclusions

In summary, we propose a promising approach to synthesis CNC-fullerene nano-composites as anti-oxidant agents. The structure of pHEMA-CNC-g-C<sub>60</sub> was characterized and the mechanisms of reactions were confirmed. By utilizing the highly effective initiator CAN and catalyst LiOH, the grafting of polymer and the conjugating of fullerene were accomplished, respectively. The anti-oxidant tests demonstrated a long-term free radical scavenging effect from pHEMA-CNC-g-C<sub>60</sub>. A single exponential decay of the reaction kinetic was obtained after subtracting the impacts from water. Hence, CNC is a good substrate for the loading of fullerene and the final product pHEMA-CNC-g-C<sub>60</sub> is a promising type of anti-aging agents with a high stability in water.

# CHAPTER 4

The theory of adsorption

---

## 4.1 Overview of adsorption

Adsorption is an adhesive process where certain kinds of molecules, atoms and ions transfer from one phase to a surface (Samuel and Osman 2013). Throughout this course of mass transfer, a film of adsorbate will be formed on the surface of adsorbents (Crittenden, et al. 2012). Generally, adsorption can be classified into physical adsorption and chemical adsorption. In addition, the surface-transfer process can be caused by the Coulombic interaction, categorized as electrostatic adsorption (Bruch, et al. 1997).

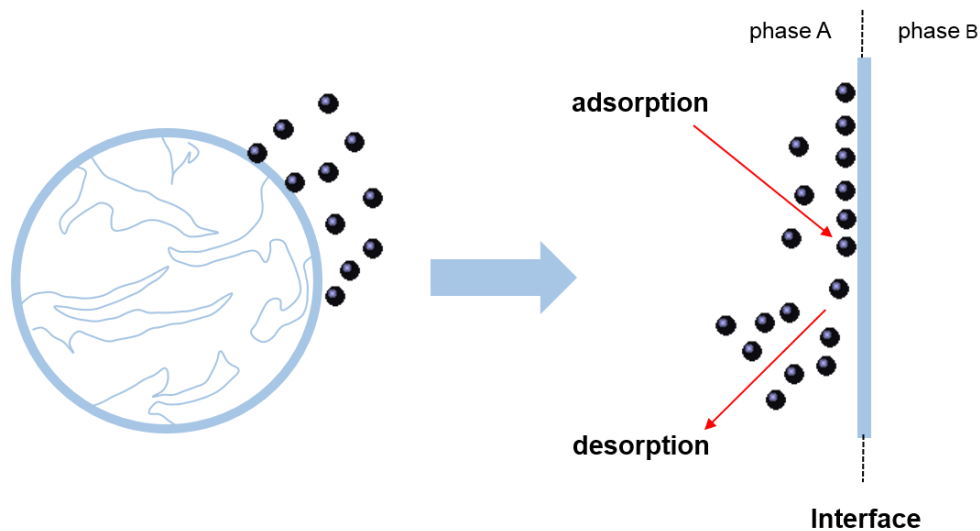


**Figure 4.1** The mass transfer between adsorbates and adsorbents

Throughout the whole process of adsorption, desorption also takes place on the surface of substrates (Harkins 1952). It is the release of substances, either from the surface of adsorbents or through the surface of adsorbents, which is the opposite of adsorption. The relative rate of adsorption and desorption, on and off the surface, determines the macro efficiency of the whole process (Toth 2002). Once the relative rate becomes zero,

adsorbents will approach the maximum adsorption capacity and system will reach its equilibrium state (Dash 2012).

From the theoretical analysis of the adsorption process, a very important parameter, the specific adsorption of an adsorbent,  $q$  (mg/g) is used to evaluate the performance of the adsorbent (Toth 2002). In liquid-solid system, it is defined as the mass of adsorbates removed from the bulk fluid and adsorbed by per mass of adsorbents (Hendricks 2006). For a batch reactor containing constant volume of liquids, the specific adsorption of an adsorbent can be calculated as follows:

$$q = \frac{(C_0 - C) \cdot V}{m} \quad (4.1)$$

$C_0$ : the initial concentration of adsorbate in the bulk fluid (mg/L)

$C$ : the concentration of adsorbate in the bulk fluid at time  $t$  (mg/L)

$m$ : the mass of the adsorbent (g)

$V$ : the total volume of the solution(L)

At equilibrium, Equation 4.1 can be modified and re-expressed as blow.

$$q_e = \frac{(C_0 - C_e) \cdot V}{m} \quad (4.2)$$

$q_e$ : the specific adsorption of an adsorbent at equilibrium (mg/g)

$C_e$ : the equilibrium concentration of the adsorbate in the bulk fluid (mg/L)

## 4.2 Modes of adsorption

The driving force of adsorption depends on the details of the species involved. Weak intermolecular forces, such as van der Waals force, provides the driving force for the physical adsorption process (Bruch, et al. 1997). Chelation and the formation of coordinating bonds are common in chemical adsorption process (Gregg, et al. 1967). Electrostatic adsorption, normally referred to as ion exchange, involves the adsorption of ions via Coulombic attractions (Gregg, et al. 1967).

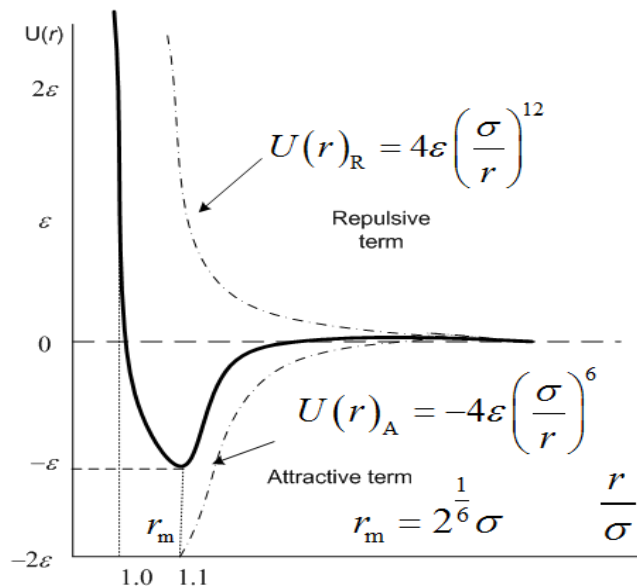


**Figure 4.2** Lennard-Jones potential (Jiang 2014)

### 4.2.1 Physical adsorption

Physical adsorption, often called physisorption, is a process in which the electronic states of bonding species were preserved with little perturbation (Oura, et al. 2003). The elemental interaction in physical adsorption is often caused by van der Waals forces. In comparison with chemical adsorption, the interaction energy of physical adsorption is

usually weak (Gregg, et al. 1967). However, the van der Waals attractions play a significant role in many natural phenomena, such as the adhesive performance of gecko (Autumn, et al. 2000). Theoretically, the van der Waals force originates from the interactions between permanent, induced or instantaneous electric dipoles (Oura, et al. 2003). In any liquid-solid system, physical adsorption is a common phenomenon, although some specific intermolecular interactions may arise from particular geometrical or electrical properties of the adsorbent and the adsorbate (Brunauer 1943). The equilibrium is established between the adsorbate on the surface of adsorbents and the bulk fluid. Due to equilibrium induced by temperature and pressure, physical adsorption process is excluded from many fields (Bruch, et al. 1997).

#### **4.2.2 Chemical adsorption**

Chemical adsorption, often called chemisorbed, involves chemical reactions between adsorbents and adsorbates. Typically, new covalent bonds are formed at specific sites on the surface of adsorbents due to the localized chemical functionality (Perry 1941). On one hand, the strong interaction between adsorbates and adsorbents creates new chemical bonds that are highly stable (Inglezakis and Pouloupoulos 2006). On the other hand, as the result of this specific interaction, there is only a monolayer of chemisorbed species and the adsorption is not reversible (Davis 2011). In terms of enthalpy change, chemical adsorption has a much greater range than physical adsorption, 40-400 kJ/mol vs 20-40 kJ/mol. It also requires activation energy and could take place at high temperature (Hendricks 2006). Accordingly, the kinetic rate of chemical adsorption may be much slower than physical

adsorption. As a result, the process of chemical adsorption may take much longer to reach equilibrium status (Ross and Morrison 1988).

	<b>Chemical adsorption</b>	<b>Physical adsorption</b>
<b>Attraction force</b>	chemical bonds	van der Waals force
<b>Temperature range</b>	virtually unlimited; a given molecule has an optimal range	below the condensation point
<b>Adsorption enthalpy</b>	wide range; high; 40-400 kJ/mol	narrow range; low; 20-40 kJ/mol
<b>Nature of adsorption</b>	maybe irreversible; often dissociative; highly specific;	reversible; non-dissociative; non-specific;
<b>Saturation uptake</b>	limited to one layer	multilayer uptake
<b>Kinetics of adsorption</b>	usually is an activated process	Fast and non-activated process

**Table 4.1** Physical adsorption vs Chemical adsorption (Alley 2007)

#### 4.2.3 Electrostatic adsorption

Electrostatic adsorption is driven by Coulombic attractions arising from the attraction of charged clouds between adsorbates and adsorbents (Noll 1991). In most cases, it may be classified as ion exchange process (Samuel and Osman 2013). Similar to chemical adsorption process, electrostatic adsorption is also a site specific process in which the excess charge is localized at specific location or functional groups. As the exchanger matrix, solid materials are able to take up charged ions from fluid and release an equivalent

amount of counter ions into the solution (Oura, et al. 2003). This interexchange process can be seen as a reversible reaction since the replacement of counter ions can occur. Hence, a number of methods can be used to regenerate adsorbents, such as strong acid for cation media, alkali for anion media (Ali and Gupta 2006). However, the capacity of adsorbents will decrease gradually due to the constant deactivation and degradation in recycle and regeneration (Ali and Gupta 2006).

### **4.3 Equilibrium adsorption isotherms**

As mentioned previously, an equilibrium between adsorption and desorption will be established after a period of time. In order to comprehensively understand the long-term process and the properties of a given system, an adsorption isotherm is used to analyze the behaviour of adsorption under constant conditions. Usually, the adsorption isotherm is a curve describing the relationship between the amount of adsorbates adsorbed onto adsorbents and the equilibrium concentration of the adsorbates in bulk fluid at a given temperature and pressure (El Qada, et al. 2006). Three classes of the most frequently used adsorption isotherms are introduced, namely: the Langmuir model, the Freundlich model and the Temkin model.

#### **4.3.1 Langmuir model**

The Langmuir isotherm was first presented by Irving Langmuir in 1916 for the adsorption of species onto a simple surface (Langmuir 1918). Initially, it was developed to describe the adsorption of gases onto clean solids. Nowadays, it has been adapted for liquid-solid system as well (Chen 2015). The isotherm is presented as follows: (1) the surface



containing the adsorbing sites is perfectly flat plane with no corrugations (assume the surface is homogeneous); (2) the adsorbing gas adsorbs to an immobile state; (3) all adsorption sites are equally favorable; (4) each site can hold at most one molecule of adsorbate (monolayer coverage only); (5) there are no interactions between adsorbed molecules on adjacent sites. The isotherm is presented in Equation 4.3 (Masel 1996).

$$q_e = \frac{q_m \cdot K_L \cdot C_e}{1 + K_L \cdot C_e} \quad (4.3)$$

$q_e$ : the specific adsorption of an adsorbent at equilibrium (mg/g)

$q_m$ : the maximum specific adsorption of an adsorbent (mg/g)

$C_e$ : the equilibrium concentration of the adsorbate in the bulk fluid (mg/L)

$K_L$ : the Langmuir affinity coefficient (L/mg)

A linear relationship of the Langmuir isotherm was derived and shown in Equation 4.4.

$$\frac{1}{q_e} = \frac{1}{K_L \cdot q_m} \cdot \frac{1}{C_e} + \frac{1}{q_m} \quad (4.4)$$

In order to obtain the maximum specific adsorption  $q_m$  and the affinity coefficient  $K_L$ , two different types of batch experiments are conducted: (1) vary the mass of adsorbent and measure the specific adsorption at equilibrium, while keeping all other parameters constant; (2) vary the initial concentration of the adsorbate in the bulk fluid and measure the specific adsorption at equilibrium, while keeping all other parameters constant; These will yield a series of values of  $C_e$  and  $q_e$  and the models parameters will be obtained using Equation 4.4.

To date, the Langmuir isotherm is the model used in almost every adsorption experiment and  $q_m$  is the essential parameter that represents the adsorption efficiency of a given material. As a result,  $q_m$  may be used to compare the performance of different materials (Quinlan 2015).

### 4.3.2 Freundlich model and Temkin model

The Freundlich and the Temkin isotherms, unlike Langmuir isotherm, are not so commonly used. Both of them are summarized in the table below (Foo and Hameed 2010).

**Table 4.2** Freundlich isotherm vs Temkin isotherm

	<b>Freundlich isotherm</b>	<b>Temkin isotherm</b>
<b>Isotherm</b>	$q_e = K_F \cdot C_e^{1/n}$	$q_e = \frac{RT}{b_T} \ln(A_T \cdot C_e)$
	$\log q_e = \log K_F + \frac{1}{n} \log C_e$	$q_e = \frac{RT}{b_T} \ln A_T + \frac{RT}{b_T} \ln C_e$
<b>Linear plot</b>	$K_F$ : an indicator of adsorption capacity; $1/n$ : an intensity measure of adsorption;	$R$ : the gas constant [J/(mol K)] $T$ : the temperature of the system (K) $b_T$ : a model parameter[g J/(mg mol)] $A_T$ : a model parameter (L/g).
<b>Assumptions</b>	Langmuir isotherm applies to each layer; no transmigration occurs between layers; an equal energy of adsorption for each layer( not the first layer); an exponential reduction in heat of adsorption;	a linear reduction in heat of adsorption; adsorption is characterized by a uniform distribution of binding energy, up to a maximum binding energy;

<b>Surfaces</b>	heterogeneous surfaces	heterogeneous surfaces
<b>Saturation uptake</b>	multilayer adsorption	multilayer adsorption
<b>limitation</b>	not applicable in low and large value of concentrations	not applicable in low and large value of concentrations
<b>Reference</b>	(Freundlich 1906)	(Temkin and Pyzhev 1940)

---

#### 4.4 Adsorption kinetics

The kinetics of adsorption are of great significance to evaluate the performance of a given adsorbent (Do 1998). The effects of different parameters and the underlying mechanisms of a given thermodynamic process can be investigated to improve the design in the adsorption model, as well as the performance of adsorbents. In the past decades, chemical engineers and mathematicians have developed several mathematical models to describe adsorption process via a series of experimental data (Toth 2002). So far, the adsorption diffusion model is the most popular (Qiu, et al. 2009). Generally, the adsorption diffusion model is comprised of three consecutive steps: (1) mass transfer from the bulk fluid to the surface of adsorbents, which is also called external diffusion, i.e., boundary layer; (2) diffusion in the liquid contained in the adsorbent, which is also called internal or intra-particle diffusion, i.e., liquid in the pores; (3) adsorption and desorption between free adsorbates and adsorbed adsorbates, i.e., adsorbate film formed on adsorbent (McKay, et al. 1981).

In order to better understand the overall process of adsorption, some of the most commonly used kinetic models are reviewed as follow.

**Table 4.3** Kinetics models of adsorption

	<b>Kinetics model</b>	<b>Linear Plot</b>	<b>Reference</b>
<b>pseudo 1<sup>st</sup> order</b>	$\frac{dq}{dt} = k_1(q_e - q)$	$\log(q_e - q) = \log q_e - \frac{k_1}{2.303}t$	(Lagergren 1898)
<b>pseudo 2<sup>nd</sup> order</b>	$\frac{dq}{dt} = k_2(q_e - q)^2$	$\frac{1}{q} = \frac{1}{k_2 q_e^2} \cdot \frac{1}{t} + \frac{1}{q_e}$	(Ho and McKay 1998)
<b>Intra-particle diffusion</b>	$q = kt^{0.5} + C$	N/A	(Weber and Morris 1963)
<b>Elovich's equation</b>	$\frac{dq}{dt} = ae^{-aq}$	$q = \frac{2.3}{\alpha} \log(t + \frac{1}{\alpha a}) - \frac{2.3}{\alpha} \log(\frac{1}{\alpha a})$	(Zeldowitsch 1934)
<b>2<sup>nd</sup> rate equation</b>	$\frac{dC_t}{dt} = -k_2 C_t^2$	$\frac{1}{C_t} = k_2 \cdot t + \frac{1}{C_0}$	(Xiong, et al. 2006)
<b>double-exponential model</b>	$q = q_e - \frac{D_1}{m_a} \exp(-K_1 t) - \frac{D_2}{m_a} \exp(-K_2 t)$	$\ln[q_e - q_t - \frac{D_2}{m_a} \exp(-K_2 t)] = \ln(\frac{D_1}{m_a}) - K_1 t$	(Wilczak and Keinath 1993)

# CHAPTER 5

Cellulose nanofibrils (CNFs) based aerogels as adsorbents to treat waste water

---

## 5.1 Introduction

The term “aerogel” was first introduced by Kistler in 1932 (Kistler 1932). In his pioneering work, a solid network was formed by replacing the liquid in the gel with air. Unlike traditional water removal process, the technique used was a new drying method, where the liquids contained in the gel was removed after being transformed to supercritical fluids. After several decades of development, aerogel is officially defined as gel comprised of microporous solid in which the dispersed phase is gas (Alemán, et al. 2006).

In the last few decades, the synthetic routes to prepare aerogels were proposed, such as the rapid supercritical extraction process (RSCE) (Aegerter, et al. 2011). Meanwhile, the choice of raw materials to form aerogels has expanded rapidly. Firstly, silica was the material of choice to fabricate aerogels. However, as the interest in aerogels has grown progressively after the 1980s, a wide range of raw materials have been used to synthesize aerogels, including tungstic oxide, cellulose, chitosan, melamine formaldehyde, ferric oxide and nickel tartrate (Fricke and Emmerling 1992). Currently, the list of candidate materials to form aerogels continues to expand.

Generally, the preparation of aerogel can be accomplished in two steps: (1) sol-gel process, in which a colloidal solution was transformed into a disorder but continuous network that is infiltrated by solvent; (2) drying or solvent removal step, in which the gel embedded in the solvent is transformed into a solvent-free network (Fricke and Emmerling 1992). In order to improve the performance of certain aerogels, a number of modifications

have been used. For example, through a low temperature hydrolysis, a higher degree of purity and homogeneity can be achieved (Woignier, et al. 1984).

Because of the abundant choices of raw materials and the highly porous structure with mechanical strength, aerogels possessing significant features have been employed for many versatile applications. Although the initial attempt to prepare aerogels from cellulose were not very successful, the cellulose based aerogel re-gained attention after Tan and coworkers reported on a cellulose based aerogel with high impact strength (Tan, et al. 2001). In their work, network gels were formed by cross-linking cellulose acetate and cellulose acetate butyrate with tolylene 2,4-diisocyanate. However, they claimed that cellulose aerogels were not adequate to form carbon aerogels due to their rapid decomposition during pyrolysis. Ironically, a type of ultralight and flexible carbon aerogels was produced by pyrolyzing bacterial cellulose foams (Wu, et al. 2013). In addition, the cellulose derived carbon aerogels displayed a high adsorption capacity and a fire-retardant property. The success of pyrolyzing cellulose leads a series of modifications on cellulose derived aerogels. For example, highly conductive and stretchable conductors were fabricated by infiltrating conductive polymers into pyrolyzed celluloses (Liang 2012). Not only in the field of electrochemistry, cellulose based aerogels have also been used as adsorbents to remove pollutants from aqueous systems. In the work of Zhao, cellulose aerogels with high porosity and large specific surface area have been used for Cr(VI) removal (Zhao, et al. 2015).

In the present work, cellulose nanofibrils (CNFs) based aerogels were used as adsorbents for the removal of heavy metal ions and synthetic dyes. In order to maintain the structure



of aerogels, the synthetic conditions were optimized. The optimized aerogels were first used to adsorb copper(II) ions, where the isotherm and kinetics of adsorption were investigated. The same procedure was applied to the removal of synthetic dyes and methyl orange (MO) was used as the model dye.

## **5.2 Experimental section**

### **5.2.1 Materials**

Cellulose nanofibrils (CNFs) with a solid content of 3.6% w/w were purchased from The Process Development Center, University of Maine. The fibrils are about 20 nm in diameter and up to 2- $\mu$ m long. Tris((hydroxymethyl)aminomethane) (Tris-), branched polyethylenimine (PEI) and dopamine hydrochloride were purchased from Sigma-Aldrich. In the study of adsorption, copper(II) sulfate pentahydrate, sodium hydroxide, hydrochloric acid, ethylenediamine and methyl orange (MO) were obtained from Sigma-Aldrich. All chemicals and solvents were used as received without further purification.

### **5.2.2 Methods**

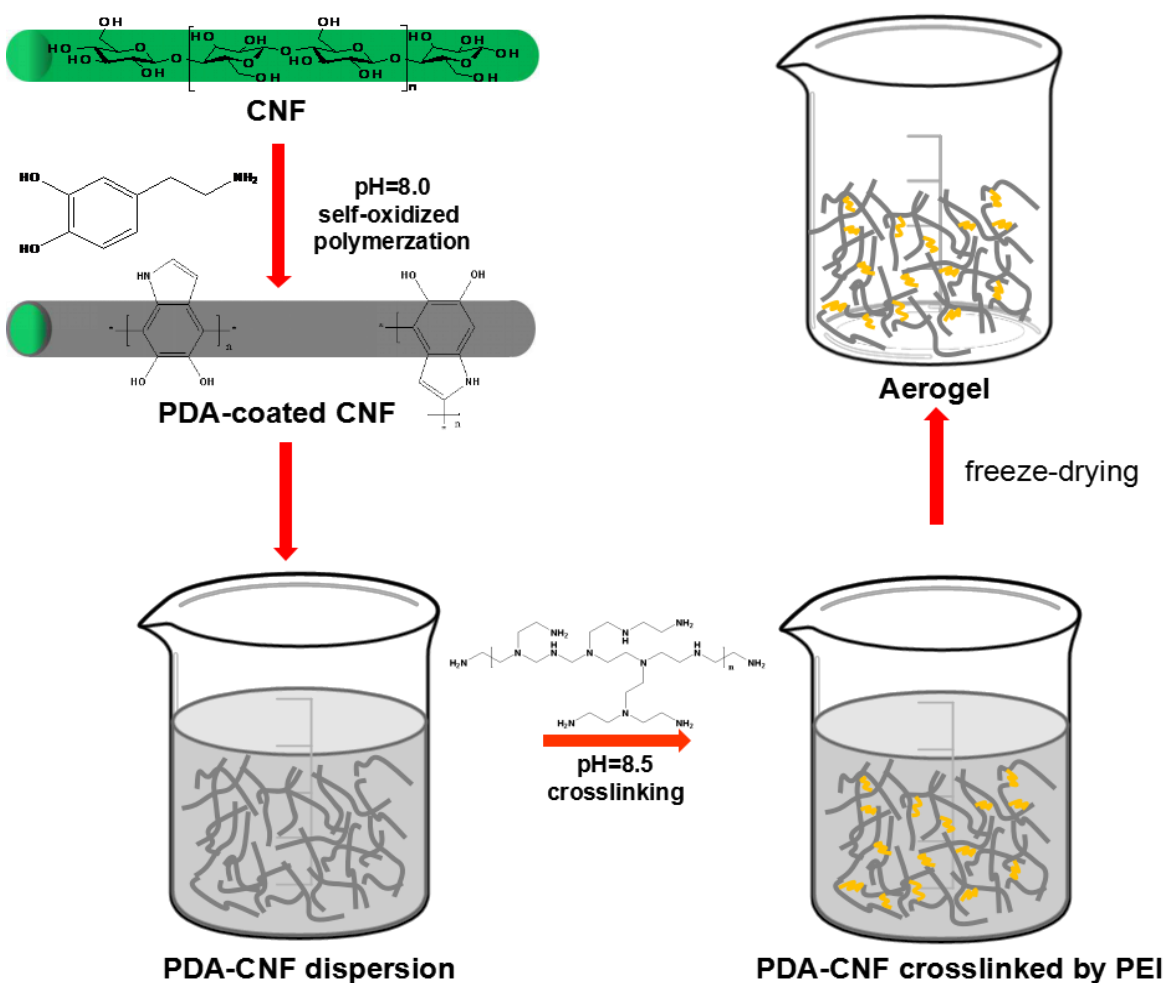
#### **5.2.2.1 Synthesis of polydopamine-CNF (PDA-CNF)**

The method to prepare PDA-CNF was adopted from a previous work of PDA-CNC (Shi, et al. 2015) (Zhang, et al. 2013). At first, 7.5 g of CNF pulp was dispersed in 400 ml Milli-Q water using an IKA T25 homogenizer. The pH was adjusted to 8.0 by adding 0.5 g of Tris-, followed by the addition of 0.5 g dopamine hydrochloride. The surface coating was performed overnight at room temperature until the suspension turned to black dispersion. The final products were purified through Büchner funnel equipped with a 20 mm pore size filtration membrane and washed with Milli-Q water several times until the filtrate became clear. After filtration, the PDA-CNF products were collected and stored.

### 5.2.2.2 Synthesis of CNF based aerogels

In the second step, 2 g of PDA-CNF (2.0% w/w) was mixed with 1 ml of PEI solution (10.0% w/w) in a 7 ml glass vial. With the help of vortex and ultra-sonication, the system was thoroughly mixed. The vial was placed in the drying oven for 2 days at 60 °C, and the CNF based aerogels were obtained after freeze drying.

The overall procedure to synthesis the CNF based aerogels is illustrated below.



Scheme 5.1 The preparation of CNF based aerogels

## 5.3 Characterizations

### 5.3.1 The mechanisms of synthesis

Dopamine was found having a similar structure with 3,4-dihydroxy-L-phenylalanine (DOPA), which is the major component responsible for the extraordinary robust adhesion performance in mussels (Liu, et al. 2014). Although the molecular structure and the polymerization mechanism of polydopamine (PDA) are still being debated, a wide range of organic and inorganic substrates including metals, ceramics and polymers were successfully coated with PDA by a simple dipping-immersing technique (Dreyer, et al. 2012) (Liebscher, et al. 2013). The same technique was adopted by Shi et al. to prepare a thin film onto CNC to stabilize colloids and silver nanoparticles (Shi, et al. 2015) (Zhang, et al. 2013). Here, the facile route to form core-shell structures was applied onto CNF. An immersion of CNF in a dilute dopamine solution, followed by tuning the pH to 8.0 caused the spontaneous polymerization of dopamine. This resulted in the formation of adhesive PDA films on the surface of CNF.

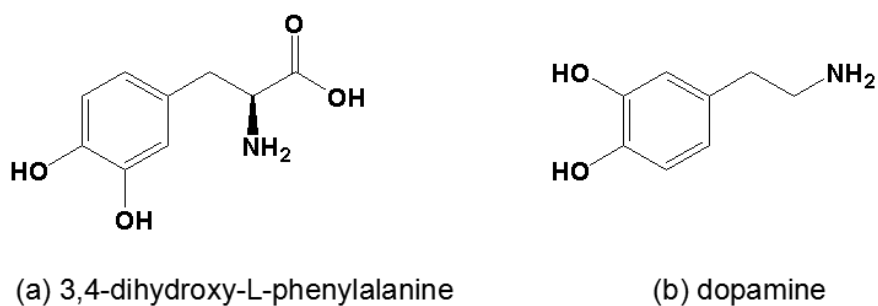


**Figure 5.1** Chemical structure of (a) DOPA and (b) Dopamine

The reaction mechanism between PDA and PEI is illustrated in Figure 5.2. When the pH value of the reaction system was raised over 8.5, the catechol groups were oxidized to

the quinone form (Lee, et al. 2007). In this case, the amine groups of PEI are able to react with the quinone form catechol groups via the Michael addition or Schiff base reaction (LaVoie, et al. 2005) (Tian, et al. 2013). Eventually, the PDA-CNFs in the system were cross-linked by the resulting covalent bonds. The structure of the cross-linked network were maintained after freeze-drying and water removal.

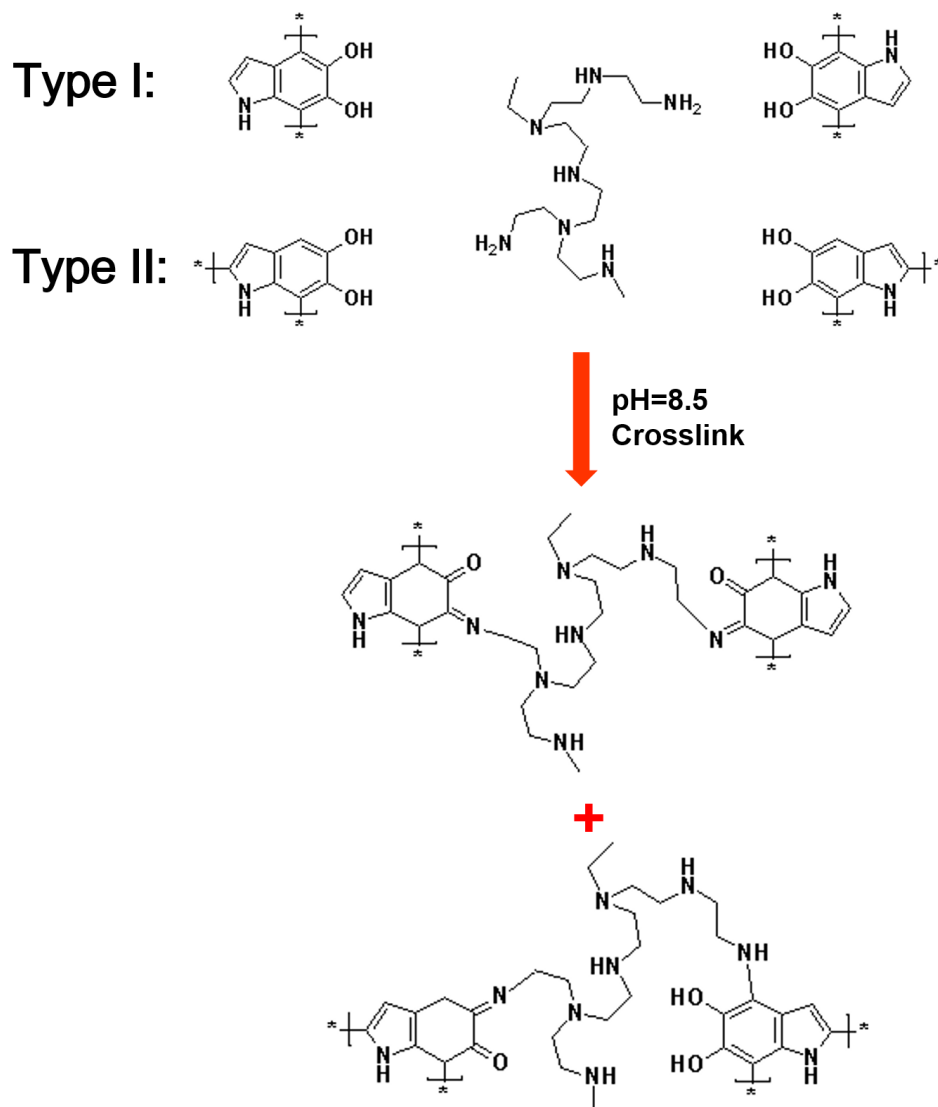


**Figure 5.2** The cross-linking reaction between PEI and PDA

### 5.3.2 Fourier Transformation Infrared Spectroscopy (FT-IR)

The aerogels were first characterized by FTIR, which is used to confirm the presence of PDA and cross-linking reaction. The peak appeared around  $1512\text{ cm}^{-1}$  in the curve of PDA-CNF can be attributed to the N-H scissoring vibrations, which indicated the successful coating of PDA (Liu, et al. 2014) (Zeng, et al. 2013). In the comparison of cross-linked PDA-CNF-PEI and physical mixed PDA-CNF-PEI, the peak around  $1657\text{ cm}^{-1}$  can be assigned to C=N stretching vibration, thereby verifying the formation of covalent bonds between PAD and PEI (Tian, et al. 2013) (Lv, et al. 2015). Hence, PEI is able to covalently bond with PDA-CNF fibrils, forming cross-linked networks.

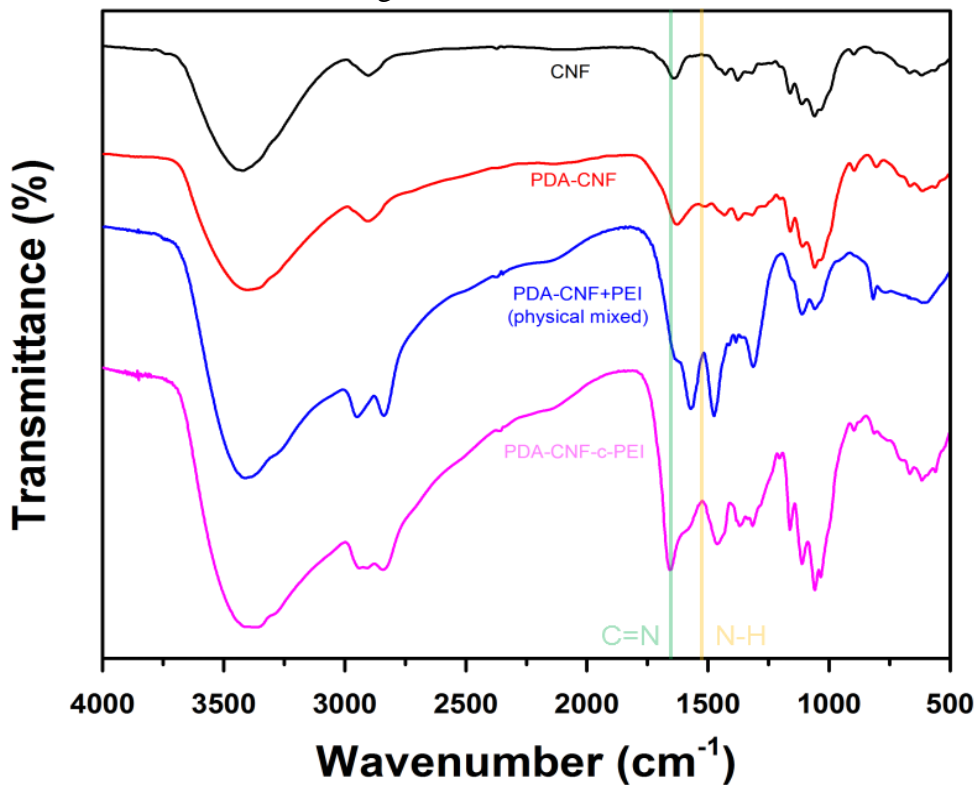
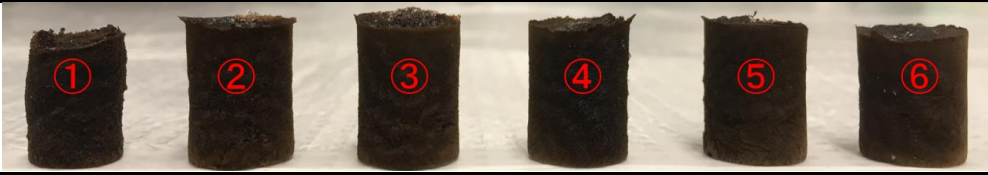








Figure 5.3 FTIR spectra of the composite aerogels

### 5.3.3 The optimization of CNF based aerogels

In order to minimize the consumption of raw materials as well as to maintain the porous structure without collapsing, two sets of comparative tests were performed.

First, the effects of the weight percent of PDA-CNF were studied with the concentration of PEI fixed at 0.05 g/ml. The weight percent of PDA-CNF was varied from 1% to 6%, resulting in a series of aerogels showed in Figure 5.4. A significant difference of the structure lies between sample No.1 and sample No.2, which indicates that, a minimum of 2.0% w/w of PDA-CNF was required to form robust aerogels.



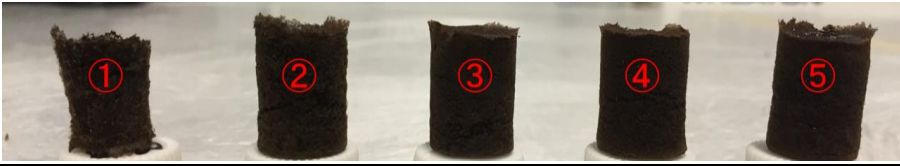
						
PDA-CNF (2 g)	1.0% w/w	2.0% w/w	3.0% w/w	4.0% w/w	5.0% w/w	6.0% w/w
PEI (0.05 g/ml)	1 ml	1 ml	1 ml	1 ml	1 ml	1 ml

**Table 5.1** CNF aerogels with different amounts of PDA-CNF

Secondly, the effects of the concentration of PEI were studied with the weight percent of PDA-CNF fixed at 2%. The concentration of PEI was varied from 0.005 g/ml to 0.045 g/ml, resulting in a set of aerogels displayed in Figure 5.5. Comparing sample No.1 and sample No.2, the difference in their structures indicated that the concentration of PEI should exceed 0.015 g/ml to completely cross-link PDA-CNF networks. Additionally, if the



concentration of PEI was further increased to 0.05 g/ml, the final aerogel will possess a compressible property as illustrated in Figure 5.6.



PDA-CNF(2 g)	2.0% w/w	2.0% w/w	2.0% w/w	2.0% w/w	2.0% w/w
PEI (1 ml)	0.005 g/ml	0.015 g/ml	0.025 g/ml	0.035 g/ml	0.045 g/ml

**Table 5.2** CNF aerogels with different concentration of PEI

In conclusion, the minimal required concentration and weight percent of PEI and PDA-CNF for maintaining the structures of aerogels are 0.015 g/ml and 2% w/w, respectively. If either of these values is lower than the minimal requirements, the resulting aerogels will collapse easily under external pressure.

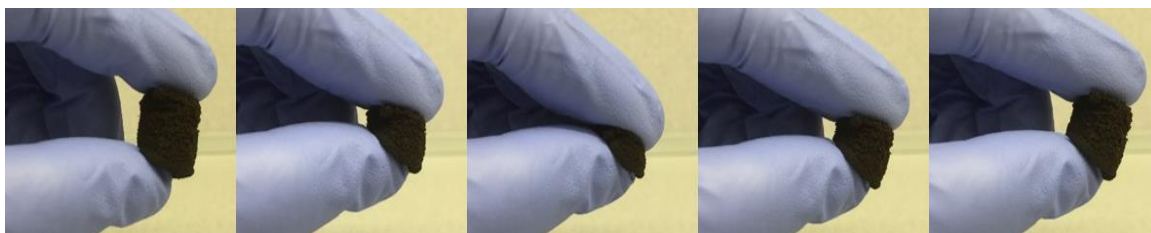


**Figure 5.4** CNF aerogels with compressible performances

### 5.3.4 The removal of methyl orange (MO)

A stock solution of 400 mg/L MO was prepared by dissolving a desired amount of MO into Milli-Q water. The stock solution was used throughout the entire course of the dye adsorption experiments. The concentration of MO was measured at a wavelength of 464 nm by UV-vis spectrophotometry (Yao, et al. 2003). A calibration curve was acquired by diluting the stock MO solution to five different concentrations and measuring the corresponding peak UV-vis absorbance (464 nm). The same calibration curve was used throughout the entire course of the adsorption experiments, converting the absorbance value of MO to its corresponding concentration.

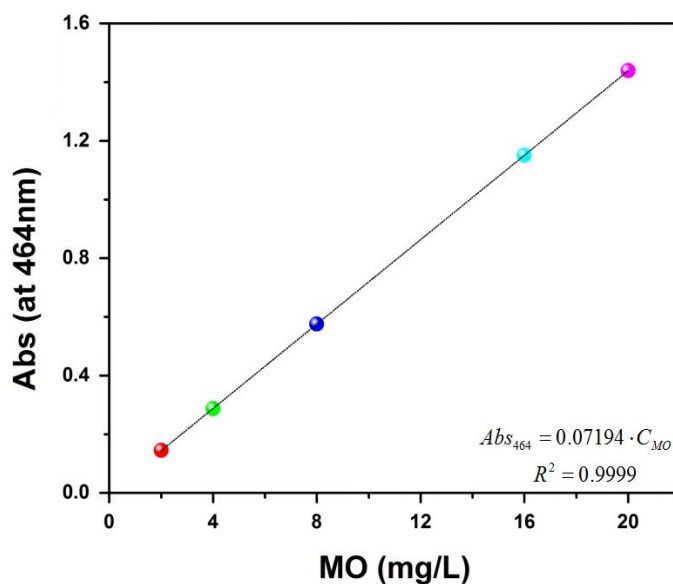


**Figure 5.5** The calibration curve of MO

### 5.3.4.1 Kinetic study of MO adsorption

The kinetics of MO adsorption was evaluated by calculating the concentration of MO solution. Specifically, a known amount of CNF aerogel was added into a centrifuge tube containing 40 ml of 200 mg/L MO solution. The tube was placed on the mixer roller at room temperature and the bulk concentration of MO was measured continuously over 11h. For each measurement, 100  $\mu$ l aliquots of bulk solution were transferred into a quartz cuvette and was diluted 20 times by adding 1.9 ml Milli-Q water, followed by UV-vis scanning.

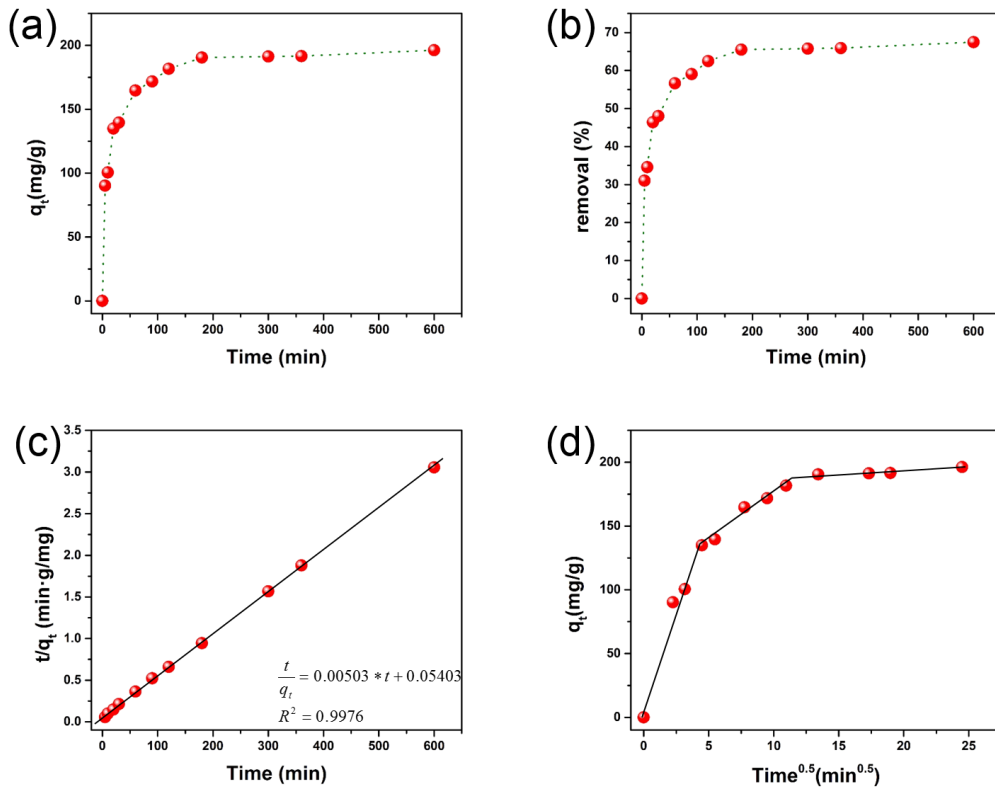


**Figure 5.6** The kinetic study of MO adsorption

(a) uptake vs time ( $q_t$  vs  $t$ ); (b) removal efficiency vs time;

(c) pseudo 2<sup>nd</sup> order model; (d) intra-particle model fitting;

The metal ions uptake  $q_t$  and the removal efficiency were plotted against time  $t$  as illustrated in Figure 5.8 (a) and 5.8 (b). The whole process was analyzed and modeled using two types of kinetics models, the pseudo 2<sup>nd</sup> order and the intra-particle diffusion model (Ho and McKay 1998) (Weber and Morris 1963). As shown in the Figure 5.8 (c), the experimental data fits in the pseudo 2<sup>nd</sup> order kinetic with an average regression coefficient  $R^2=0.9976$ . Meanwhile, the  $q_e$  calculated from the linear regression was very close to the experimental results.

On the other hand, the adsorption process involves three stages of transportation and diffusion, namely (1) external diffusion: MO molecules diffused from bulk solution to the surface of aerogels, which is the most rapid step; (2) internal diffusion: MO molecules start to enter pores of adsorbent once the surface of aerogels becomes saturated, which is slower than the first step; (3) equilibrium: the equilibrium of the MO adsorption process was achieved. According to this theory, the kinetic rates should display a trend,  $k_{id.1}>k_{id.2}>k_{id.3}$ , which is in agreeance with Figure 5.8 (d) (Mohammed, et al. 2015).

Here, two mathematical models were used to elucidate the dynamic process of adsorption and the MO adsorption experiment fits both of models

pseudo 2 <sup>nd</sup> order model	$q_e$ (exp)		$q_e$ (calc)		$R^2$	
	mg/g		mg/g			
	196.30		198.80		0.9998	
intra-particle model	$K_{id.1}$	$R_1^2$	$K_{id.2}$	$R_2^2$	$K_{id.3}$	$R_3^2$
	mg/(g min <sup>0.5</sup> )		mg/(g min <sup>0.5</sup> )		mg/(g min <sup>0.5</sup> )	

---

32.10217	0.9848	7.47851	0.9882	0.20883	0.9987
----------	--------	---------	--------	---------	--------

---

**Table 5.3** Parameters in pseudo 2<sup>nd</sup> order model and intra-particle model

### 5.3.4.2 Equilibrium adsorption of MO

In order to obtain the  $q_m$  and  $K_L$ , a series of batch adsorption experiments were carried out as follows: (1) five batch experiments were prepared by transferring 10ml of stock MO solution into each 20ml polypropylene vial; (2) to each, different amounts of CNF based aerogels were added and the vials were immediately placed on a roller mixer; (3) the equilibrium was achieved after 6h, 200  $\mu$ l aliquots of MO solution was removed from each vial and diluted 20 times by adding 3.8 ml Milli-Q water; (4) the diluted solution was scanned under UV-vis spectrophotometer and the final concentrations of each vial were obtained using the calibration curve.

The equilibrium adsorption of MO onto CNF based aerogels was modeled using the Langmuir isotherm (Langmuir 1918). As illustrated in the Figure 5.8, the maximum adsorption capacity of the CNF aerogels was calculated to be 265.9 mg/g.

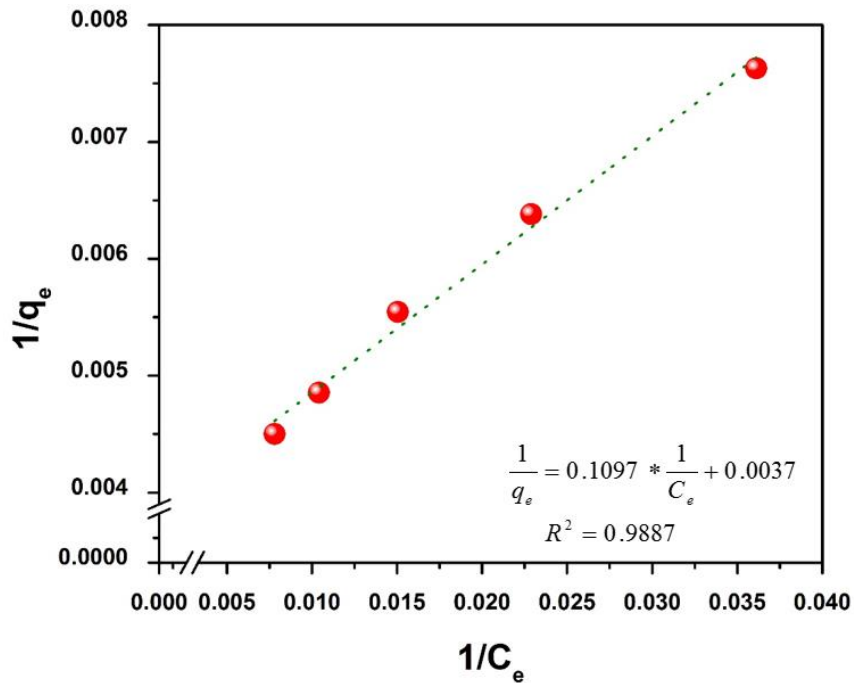


**Figure 5.7** The linearized plot for adsorption of MO onto CNF aerogels

### 5.3.4.3 The effects of pH on MO adsorption

As the pH was increased from 4 to 10, the maximum adsorption capacity decreased from 265.9 mg/g to 218.3 mg/g. The results showed that the CNF based aerogels can maintain a high adsorption capacity over a wide pH range. The pH value played a key role in tailoring the surface charge of CNF aerogels due to the protonation and deprotonation of amine and amino groups. At low pH, the aerogels possess positive charges, which attract the negatively charged MO. At high pH, the positive charge on the aerogels surface decreased that resulted in a reduction of adsorption capacity.

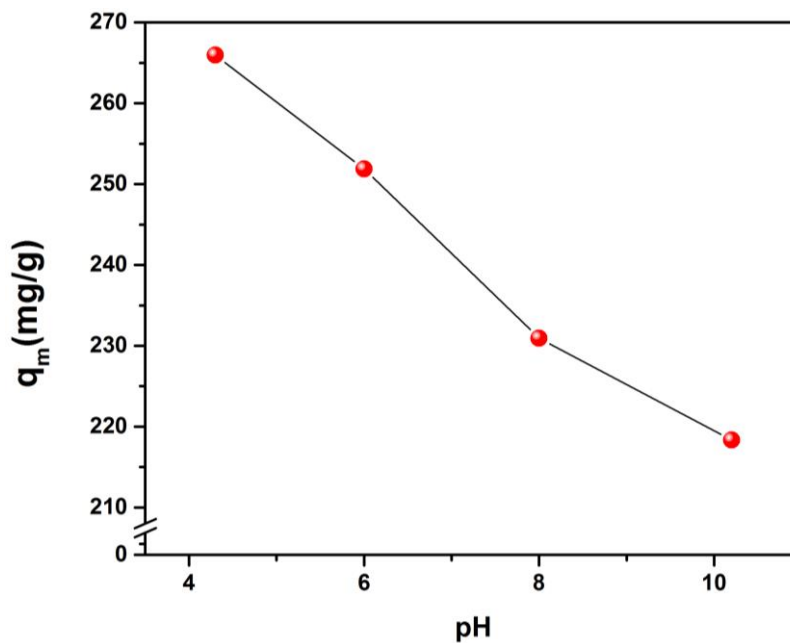


**Figure 5.8** The effects of pH on the adsorption of MO onto CNF aerogels



### 5.3.5 The removal of Cu<sup>2+</sup>

A stock solution of 1 mol/L CuSO<sub>4</sub> was prepared. The stock solution was used throughout the entire course of Cu<sup>2+</sup> adsorption experiments. The concentration of Cu<sup>2+</sup> was measured with ethylenediamine via UV-vis spectrophotometry (Zhang, et al. 2011). The complex formed from Cu<sup>2+</sup> and ethylenediamine possesses a UV absorbance peak at 557 nm (Yang, et al. 2013). A calibration curve was obtained by diluting the stock CuSO<sub>4</sub> solution to five different concentrations and measuring the corresponding UV-vis absorbance peak (557 nm) with the addition of ethylenediamine. The same calibration curve was used throughout the course of the adsorption experiments.

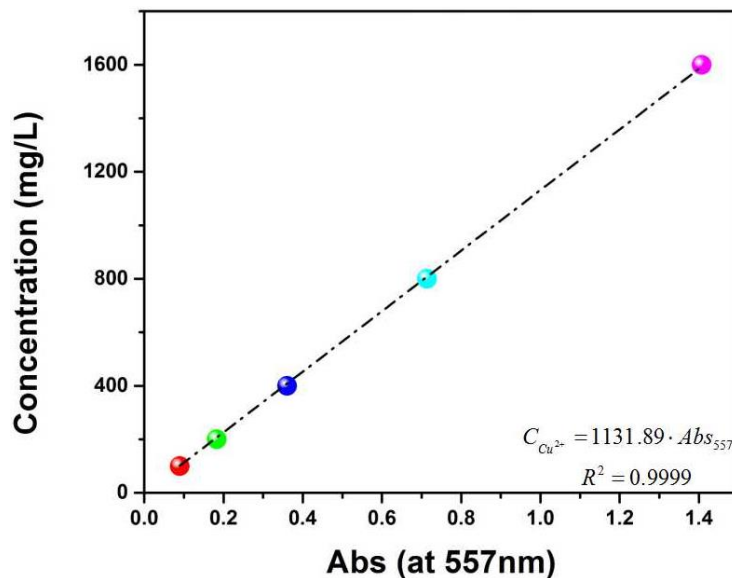


**Figure 5.9** The calibration curve of Cu<sup>2+</sup>/ethylenediamine complex

### 5.3.5.1 Kinetic study of $\text{Cu}^{2+}$ adsorption

The kinetics of  $\text{Cu}^{2+}$  adsorption was evaluated by measuring the concentration of the  $\text{Cu}^{2+}$ /ethylenediamine complex. Specifically, a certain amount of CNF aerogel was added to a polypropylene vial containing 20 ml of 1000 ppm  $\text{Cu}^{2+}$  solution. The vial was placed on a mixer roller at room temperature and the bulk concentration of  $\text{Cu}^{2+}$  was measured continuously over 15 h. For each measurement, 100  $\mu\text{l}$  aliquots of bulk solution were transferred into a quartz cuvette and mixed with 5  $\mu\text{l}$  of ethylenediamine, followed by UV-vis scanning.

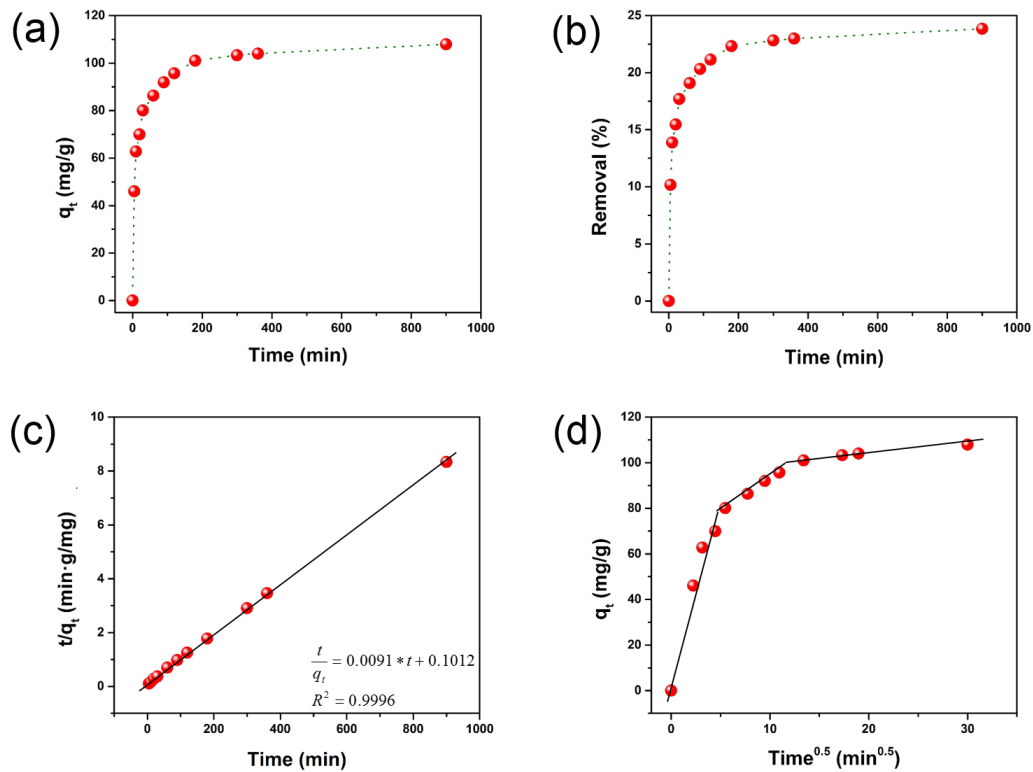


**Figure 5.10** The kinetic study of  $\text{Cu}^{2+}$  adsorption

(a) uptake vs time ( $q_t$  vs  $t$ ); (b) removal efficiency vs time;

(c) pseudo 2<sup>nd</sup> order model; (d) intra-particle model fitting;

The metal ion uptake  $q_t$  and the removal efficiency were plotted against time  $t$  as illustrated in Figure 5.12 (a) and 5.12 (b). This whole process was analyzed and modeled using two types of kinetics models, the pseudo 2<sup>nd</sup> order and the intra-particle diffusion model (Ho and McKay 1998) (Weber and Morris 1963). As shown in the Figure 5.12 (c), the experimental data fits in the pseudo 2<sup>nd</sup> order kinetic with an average regression coefficient  $R^2=0.9996$ . Meanwhile, the  $q_e$  calculated from the linear regression was very close to the experimental results.

On the other hand, the adsorption process involves three stages of transportation and diffusion, namely (1) external diffusion: the diffusion of  $\text{Cu}^{2+}$  ions from bulk solution to the surface of aerogels, which is the most rapid step; (2) internal diffusion: the entry of  $\text{Cu}^{2+}$  ions into pores of the adsorbents once the surface of aerogels becomes saturated, which is slower than the first step; (3) equilibrium: the achievement of equilibrium in the  $\text{Cu}^{2+}$  adsorption process. According to this theory, the kinetic rates should display a trend,  $k_{id.1} > k_{id.2} > k_{id.3}$ , which is in agreeance with Figure 5.12 (d) (Mohammed, et al. 2015).

Here, two mathematical models were used to describe the dynamic process of adsorption and the  $\text{Cu}^{2+}$  adsorption experiment fit both models.

pseudo 2 <sup>nd</sup> order model	$q_e$ (exp)		$q_e$ (calc)		$R^2$	
	mg/g		mg/g			
	107.93		109.05		0.9996	
intra-particle model	$K_{id.1}$	$R_1^2$	$K_{id.2}$	$R_2^2$	$K_{id.3}$	$R_3^2$
	mg/(g min <sup>0.5</sup> )		mg/(g min <sup>0.5</sup> )		mg/(g min <sup>0.5</sup> )	

---

17.5561	0.9791	2.8923	0.9978	0.4004	0.9738
---------	--------	--------	--------	--------	--------

---

**Table 5.4** Parameters in pseudo 2<sup>nd</sup> order model and intra-particle model

### 5.3.5.2 Equilibrium adsorption

In order to obtain the  $q_m$  and  $K_L$ , a series of batch adsorption experiments was carried out as follows: (1) five batch experiments were prepared by transferring 10ml of 500 ppm  $\text{Cu}^{2+}$  solution into each 20ml polypropylene vial; (2) to each, different amounts of CNF based aerogels were added and the vials were immediately placed on a roller mixer; (3) the equilibrium was achieved after 6h, 2 ml aliquots of MO solution was removed from each vial and mixed with 100  $\mu\text{l}$  aliquots ethylenediamine solution; (4) the mixed solution containing  $\text{Cu}^{2+}$ /ethylenediamine complexes was scanned in a UV-vis spectrophotometer and the final concentrations of each vial were obtained via the calibration curve.

The equilibrium adsorption of  $\text{Cu}^{2+}$  onto CNF based aerogels was modeled using the Langmuir isotherm (Langmuir 1918). As illustrated in the Figure 5.13, the maximum adsorption capacity of the CNF aerogels was calculated to be 103.5 mg/g.

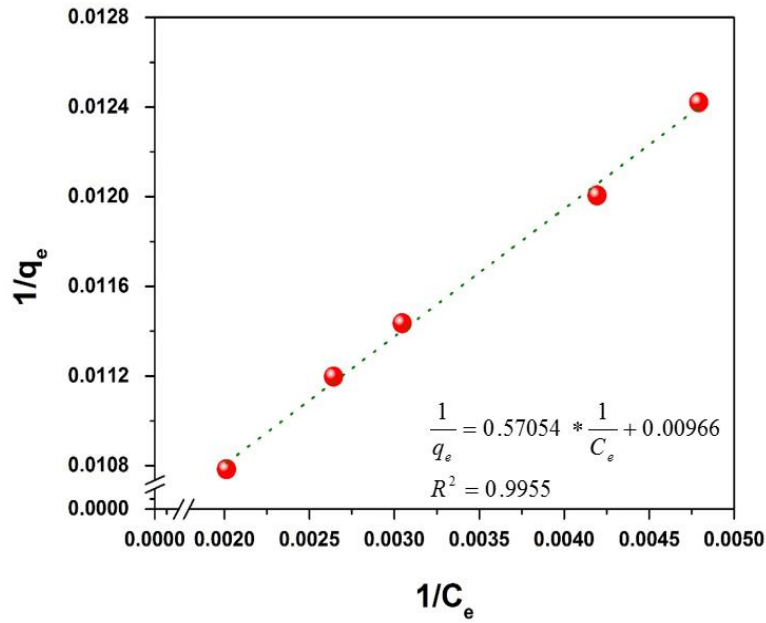


**Figure 5.11** The linearized plot for adsorption of  $\text{Cu}^{2+}$  onto CNF aerogels

### 5.3.5.3 The effects of pH on Cu<sup>2+</sup> adsorption

In a solution of high pH, copper(II) ions form precipitates or complexes with hydroxide ions (Lee, et al. 2006). So, the effect of pH on the adsorption of Cu<sup>2+</sup> was evaluated in the range of 3 to 5. As the pH was decreased from 5 to 3, the maximum adsorption capacity decreased from 103.5 mg/g to 56.9 mg/g. In acidic solution, the protonated amine groups can bind cupric ions. However, if the value of pH is too low, the large amounts of H<sup>+</sup> may compete with metal ions for the binding sites. Additionally, the catechol groups of PDA have a strong propensity to coordinate with Cu<sup>2+</sup> and the structure of PDA may be altered in very acid conditions (El Qada, et al. 2012). Moreover, the increasing electrostatic repulsion between positively charged adsorbates and positively charged adsorbents reduces the adsorption (Yu, et al. 2014). Hence, the reduction of pH would result in a decrease in the maximum adsorption capacity.

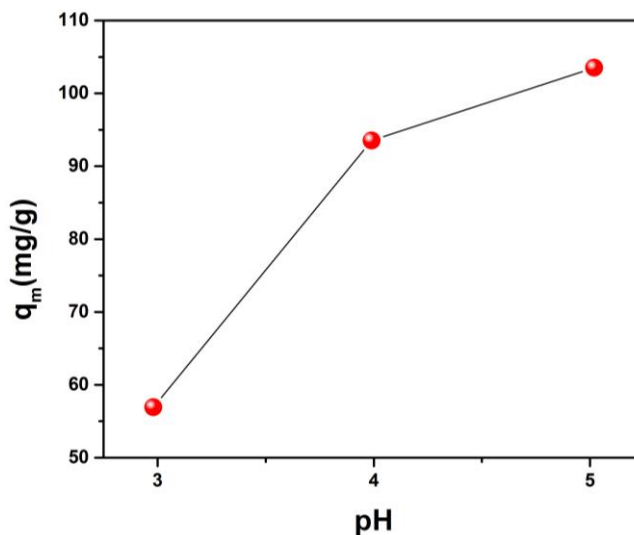


**Figure 5.12** The effects of pH on the adsorption of Cu<sup>2+</sup> onto CNF aerogels

## 5.4 Conclusions

The disintegrated product from plant cellulose CNF could be easily converted to aerogel with controllable density. The crosslinked 3D networks with high porosity are highly effective for the adsorption of methyl orange and copper(II) ions. In the study of adsorption, both kinetics and isotherm process could be adequately described by the proposed mathematical models. The results of the present study showed that CNF based aerogel has considerable potentials for the removal of MO and  $\text{Cu}^{2+}$ . The maximum adsorption capacity for MO and  $\text{Cu}^{2+}$  are 265.9 mg/g and 103.5 mg/g, respectively. Hence, CNF based aerogels with attractive features, such as low cost, compressibility, sustainability, high adsorption capacity and easy to fabricate, can be considered as commercially viable adsorbents.

Adsorbent	Capacity (mg/g)	Kinetic model	Isotherm	Reference
chitosan-cotton fiber	24.8	pseudo 2 <sup>nd</sup> order	Langmuir	(Zhang, et al. 2008)
chitosan-cellulose	26.5	pseudo 2 <sup>nd</sup> order	Langmuir	(Sun, et al. 2009)
rice husk-tartaric acid	31.8	N/A	Langmuir	(Wong 2003)
wheat bran	51.5	N/A	Langmuir	(Özer, et al. 2004)
coirpith carbon	39.7	pseudo 1 <sup>st</sup> order	Langmuir	(Namasivayam and Kadirvelu 1997)
cassava bark waste	90.9	pseudo 2 <sup>nd</sup> order	Langmuir	(Horsfall, et al. 2006)

**Table 5.5** Different kinds of biomass based adsorbent for the removal of Cu<sup>2+</sup>

Adsorbent	Capacity mg/g	Kinetic model	Isotherm	Reference
de-oiled soya	16.66	pseudo 1 <sup>st</sup> order	Langmuir	(Mittal, et al. 2007)
silkworm exuviae	87.03	pseudo 2 <sup>nd</sup> order	Langmuir	(Chen, et al. 2011)
bagasses fly ash	18.8	pseudo 2 <sup>nd</sup> order	Langmuir	(Mall, et al. 2006)
banana peel	21	intra-particle diffusion	Langmuir	(Annadurai, et al. 2002)
chitosan	34.83	pseudo 2 <sup>nd</sup> order	Langmuir	(Tapan Kumar 2010)
chitin	107.5	N/A	Langmuir	(Li, et al. 2010)

**Table 5.6** Different kinds of biomass based adsorbent for the removal of MO



# CHAPTER 6

Conclusions and recommendations for future study

---

## 6.1 Conclusions for the study presented in chapter 3

The anti-aging product, pHMEA-CNC-g-C<sub>60</sub>, was prepared using a two-spot synthesis. In this design, CAN was used as the initiator and free radical producer to accomplish the grafting of pHEMA onto CNC (Gupta and Sahoo 2001). The resulting pHMEA-CNCs laid the base for the next step, where fullerenes were covalently immobilized onto pHMEA-CNCs using LiOH as the catalyst. On one hand, the primary hydroxyl groups on CNC were conserved after the polymer grafting and fullerene still have the chance to directly conjugate onto CNCs (Kan, et al. 2013). On the other hand, contributed to the pHMEA, fullerenes have more spaces and sites for the conjugating reaction with hydroxyl groups. Meanwhile, with the introduction of CNC, the  $\pi$ - $\pi$  stacking induced aggregation behaviour of fullerenes can be largely diminished. The excellent stability in water indicated that the introduction of CNC is a desirable way to synthesize water-processable fullerene derivatives.

The final products were first characterized using FIIR. The spectra of pristine CNC, pHMEA-CNC and pHMEA-CNC-g-C<sub>60</sub> were obtained. Comparing pristine CNC with pHMEA-CNC, the presence of polymers can be confirmed. From the spectrum of pHMEA-CNC-g-C<sub>60</sub>, four characteristic peaks of fullerene appeared, indicating a fullerenes containing system. However, the results from this technique cannot provide information on reaction mechanisms.

Secondly, <sup>1</sup>H-NMR was used to verify the conjugating reaction between fullerenes and hydroxyl groups. The data obtained from this technique was used to demonstrate the

proposed reaction mechanisms. Briefly, LiOH is a suitable catalyst to facilitate the conjugation reaction between fullerenes and hydroxyl groups.

Thirdly, the grafting degree of fullerenes onto pHMEA-CNC was obtained through TGA. Pristine fullerene showed an excellent thermal stability throughout the whole period of pyrolysis (20 °C -800 °C) while pHMEA-CNC started to decompose around 190 °C. Based on the differences from the residues, the grafting degree was calculated to be 46.3%. Hence, LiOH is highly effective in the conjugating reaction.

Lastly, the anti-oxidant performance was tested using DPPH as the free radical model. A pseudo 1<sup>st</sup> order kinetic model was desired to describe the performance of free radical scavenging of pHMEA-CNC-g-C<sub>60</sub>. In order to fit in the chosen model, initial concentrations of pHMEA-CNC-g-C<sub>60</sub> and DPPH were tuned. From the spectra of UV-vis scanning over 200 mins, a linear kinetic curve was achieved and the reaction rate was calculated to be 0.008 min<sup>-1</sup>.

In conclusion, CNC is a good substrate for the loading of fullerene and the final product pHMEA-CNC-g-C<sub>60</sub> is a promising type of anti-aging agents with a high stability in water.

## 6.2 Conclusions for the study presented in chapter 5

A bioinspired polymer, polydopamine, was employed to assist the formation of CNF based aerogels. Firstly, the facile method to prepare PDA coated CNC was adopted to prepare PDA coated CNF (Shi, et al. 2015). The flexibility and the adaptability of CNF were maintained after the coating of polymers. Then, PDA-CNFs were crosslinked by PEI via the Michael addition and Schiff base reaction (LaVoie, et al. 2005) (Tian, et al. 2013). The resulting 3D networks were very robust in water after freeze-drying.

First of all, the ratio between PDA-CNF and PEI was optimized to achieve a minimum consumption of raw materials. In order to form robust aerogels, a minimum of 2.0% w/w of PDA-CNF was required and the concentration of PEI should exceed 0.015 g/ml. Appealingly, the resulting aerogels displayed compressible and stretchable properties under external pressures.

Later on, the aerogels were used to remove MO from water. The kinetic study was investigated at first. By continuously measuring the bulk concentration of MO over 11 h, the relationship between uptake of MO and time can be obtained. Two mathematical models were used to elucidate the dynamic process of adsorption and the MO adsorption experiment fits both of them (Ho and McKay 1998) (Weber and Morris 1963). In the fitting of pseudo 2<sup>nd</sup> order model, the experimental value of  $q_e$  was very close to the value of  $q_e$  calculated from linear regressions. In the fitting of intra-particle diffusion model, the kinetic rates displayed a trend,  $k_{id.1} > k_{id.2} > k_{id.3}$  (32.10217 > 7.47851 > 0.20883), which was in agreement with the diffusion theory.

The investigation for equilibrium adsorption isotherm was conducted immediately after the kinetic study. Five batch experiments was conducted to obtain the relationship between the adsorbent mass and the equilibrium concentration of MO in the bulk fluid. After modeling using Langmuir isotherm, the maximum adsorption capacity of the CNF based aerogels was calculated to be 265.9mg/g (Langmuir 1918).

At last, the effects of pH was investigated. The results showed that the CNF based aerogels can maintain a high adsorption capacity over a wide pH range. Even at pH=10.0 aqueous phase, the maximum adsorption capacity of the CNF based aerogels was still higher than 200 mg/g.

Following section was the removal of  $\text{Cu}^{2+}$  from water. The kinetic study was conducted at first. By indirectly measuring the bulk concentration of  $\text{Cu}^{2+}$  for continuous 15 h via the complex of  $\text{Cu}^{2+}$ /ethylenediamine, the relationship between uptake of  $\text{Cu}^{2+}$  and time can be obtained. Two mathematical models were used to elucidate the dynamic process of adsorption and the  $\text{Cu}^{2+}$  adsorption experiment fits both of them (Ho and McKay 1998) (Weber and Morris 1963). In the fitting of pseudo 2<sup>nd</sup> order model, the experimental value of  $q_e$  was very close to the value of  $q_e$  calculated from linear regressions. In the fitting of intra-particle diffusion model, the kinetic rates displayed a trend,  $k_{id.1} > k_{id.2} > k_{id.3}$  (17.5561 > 2.8923 > 0.4004), which was in agreeance with the diffusion theory.

The investigation for equilibrium adsorption isotherm was conducted immediately after the kinetic study. Five batch experiments was conducted to obtain the relationship between the adsorbent mass and the equilibrium concentration of  $\text{Cu}^{2+}$  in the bulk fluid. After

modeling using the Langmuir isotherm, the maximum adsorption capacity of the CNF based aerogels was calculated to be 103.5 mg/g (Langmuir 1918).

At last, the effects of pH was investigated. As the pH was decreased from 5 to 3, the maximum adsorption capacity decreased from 103.5 mg/g to 56.9 mg/g. The reduction in the maximum adsorption capacity can be explained by several reasons. If the value of pH is too low, metal ions may have to compete with large amounts of  $H^+$  for the binding sites. Meanwhile, the structure of PDA might be altered in acidic conditions (El Qada, et al. 2012). As a result, the performance of PDA to coordinate with  $Cu^{2+}$  was strongly disturbed. Moreover, the increasing electrostatic repulsion between positively charged adsorbates and positively charged adsorbents reduces the adsorption capacity (Yu, et al. 2014).

To the best of our knowledge, this type of CNF based aerogels showed advantages in the removal of MO and  $Cu^{2+}$  over other types of biomass based materials. In summary, it can be considered as commercially viable adsorbents.

### **6.3 Recommendations for future study relevant to the work in chapter 3**

#### 1. Investigate the relationship between graft degree and stability in water

The grafting degree of fullerenes onto pHEMA-CNC can be approached up to 46.3% utilizing LiOH. Based on the observation of obtained pHEMA-CNC-g-C<sub>60</sub>, the grafting degree could be able to increase further without impairing the stability in water. Meanwhile, the grafting ratio of pHEMA onto CNC can be investigated. By doing this, an optimized anti-oxidant nanomaterials could be produced.

#### 2. Investigate other applications for this nanocomposites

As mentioned in chapter 2 - Literature review, fullerene with such as a unique structure has the potential to be used in a wide range of fields, including solar cell, photoluminescence, tumor targeting and drug delivery. In recent years, the interest in photoluminescent fullerene particles has grown rapidly. For instance, in the work of Jeong *et al.*, the same catalyst LiOH was used to conjugate fullerenes with tetraethylene glycol (TEG) (Jeong, et al. 2012). The color of photoluminescent C<sub>60</sub>-TEG particles can be tuned by varying the initial concentration of fullerenes and the extent of oxidation.

## 6.4 Recommendations for future study relevant to the work in chapter 5

### 1. Tune the ratio between PDA-CNF and PEI for the adsorption of MB

Polydopamine is a well-known polymer for the removal of methylene blue (MB). There are several adsorption interactions between PDA and MB, including electrostatic interaction,  $\pi$ - $\pi$  stacking interaction and chemical reaction (Fu, et al. 2015) (Wang, et al. 2015). Unfortunately, a higher cross-linking degree will reduce the active sites on PDA for the adsorption of MB since covalent bonds were formed between PEI and PDA through on same sites. By varying the amount of PEI, resulting CNF aerogels may display a good adsorption capacity towards MB. In this case, CNF based aerogels could be used to remove different kinds of synthetic dyes.

### 2. Investigate adsorption on other heavy metal ions

Besides Cu(II) ions, a wide range of heavy metal ions can be adsorbed onto PDA and PEI (Wu, et al. 2015). For example, the effects of the concentration of PEI on the adsorption of chromium ions ( $\text{Cr}^{4+}$ ) were investigated by Aroua et al. (Aroua and Zuki 2007). Additionally, the concentration of Cr(VI) can be measured with 1,5-diphenylcarbazide via UV-vis spectrophotometry. The complex formed from  $\text{Cr}^{4+}$  and 1,5-diphenylcarbazide possessed a UV absorbance peak at 540 nm (Wang, et al. 2010).

### 3. Investigate other applications for CNF based aerogels

It is well-known that cellulose based aerogels can be used as separation media for oil-water mixtures (Cervin, et al. 2012). Highly porous structure and superhydrophobic surface



are the key factors to successfully manufacture these separation media (Korhonen, et al. 2011). In the work presented in chapter 5, CNF based 3D networks were produced. Hence, the robust aerogels can be used as structure frame to support other hydrophobic materials via coating or grafting methods. Furthermore, if CNF can be replaced by CNC, an ultra-light and highly porous 3D structure can be obtained.

# References

- Aburjai, T., and F. M. Natsheh. 2003. "Plants used in cosmetics." *Phytotherapy Research* 987-1000.
- Aegerter, M. A., N. Leventis, and M. M. Koebel. 2011. *Aerogels handbook*. Springer Science & Business Media.
- Alemán, J., J. He, M. Hess, and R. G. Jones. 2006. "Definitions of terms relating to the structure and processing of sols, gels, networks, and inorganic-organic hybrid materials ." *IUPAC Provisional Recommendations For Peer Review Only*.
- Ali, I., and V. K. Gupta. 2006. "Advances in water treatment by adsorption technology." *Nature protocols* 2661-2667.
- Alley, E. R. 2007. *Water quality control handbook*. New York: McGraw-Hill.
- Annadurai, G., R. S. Juang, and D. J Lee. 2002. "Use of cellulose-based wastes for adsorption of dyes from aqueous solutions." *Journal of Hazardous Materials* 263-274.
- Araki, J., M. Wada, S. Kuga, and T. Okano. 2000. "Birefringent glassy phase of a cellulose microcrystal suspension." *Langmuir* 2413-2415.

- Aroua, M. K., and F. M. Zuki. 2007. "Removal of chromium ions from aqueous solutions by polymer-enhanced ultrafiltration." *Journal of Hazardous Materials* 752-758.
- Autumn, K., Y. A. Liang, S. T. Hsieh, W. Zesch, W. P. Chan, T. W. Kenny, and R. J. Full. 2000. "Adhesive force of a single gecko foot-hair." *Nature* 681-685.
- Azizi Samir, M. A. S., F. Alloin, and A. Dufresne. 2005. "Review of recent research into cellulosic whiskers, their properties and their application in nanocomposite field." *Biomacromolecules* 616-626.
- Bailey, S. E., T. J. Olin, R. M. Bricka, and D. D. Adrian. 1999. "A review of potentially low-cost sorbents for heavy metals." *Water research* 2469-2479.
- Balmer, J. M., K. Fukukawa, and E. R. Gray. 2007. "The nature and management of ethical corporate identity: A commentary on corporate identity, corporate social responsibility and ethics." *Journal of Business Ethics* 7-15.
- Belfer, S., R. Fainshtain, Y. Purinson, J. Gilron, M. Nyström, and M. & Mäntt äri. 2004. "Modification of NF membrane properties by in situ redox initiated graft polymerization with hydrophilic monomers." *Journal of membrane science* 55-64.
- Bezmelnitsin, V. N., A. V. Eletsii, and E. V. Stepanov. 1994. "Cluster origin of fullerene solubility." *The Journal of Physical Chemistry* 6665-6667.

- Blöcher, C., J. Dorda, V. Mavrov, H. Chmiel, N. K. Lazaridis, and K. A. Matis. 2003. "Hybrid flotation—membrane filtration process for the removal of heavy metal ions from wastewater." *Water Research* 4018-4026.
- Bondet, V. 1997. "Kinetics and mechanisms of antioxidant activity using the DPPH. free radical method." *LWT-Food Science and Technology* 609-615.
- Bontempo, D., K. L. Heredia, B. A. Fish, and H. D. Maynard. 2004. "Cysteine-reactive polymers synthesized by atom transfer radical polymerization for conjugation to proteins." *Journal of the American Chemical Society* 15372-15373.
- Braun, B., and J. R. Dorgan. 2008. "Single-step method for the isolation and surface functionalization of cellulosic nanowhiskers." *Biomacromolecules* 334-341.
- Bruch, L. W., M. W. Cole, and E Zaremba. 1997. *Physical adsorption: forces and phenomena*. Oxford University Press.
- Brunauer, S. 1943. *Physical adsorption*. PUP.
- Cervin, N. T., C. Aulin, P. T. Larsson, and L. Wågberg. 2012. "Ultra porous nanocellulose aerogels as separation medium for mixtures of oil/water liquids." *Cellulose* 401-410.
- Chaudhri, S. K., and N. K. Jain. 2009. "History of cosmetics." *Asian Journal of Pharmaceutics* 164.

- Chen, H., J. Zhao, J. Wu, and G. Dai. 2011. "Isotherm, thermodynamic, kinetics and adsorption mechanism studies of methyl orange by surfactant modified silkworm exuviae." *Journal of hazardous materials* 246-254.
- Chen, X. 2015. "Modeling of Experimental Adsorption Isotherm Data." *Information* 14-22.
- Chequer, F. M. D., D. P. de Oliveira, E. R. A. Ferraz, G. A. R. de Oliveira, J. C. Cardoso, and M. V. B. Zanoni. 2013. *Textile dyes: dyeing process and environmental impact*. INTECH Open Access Publisher.
- Cope, S. E. 2003. "Effective retexturization of the skin, producing significantly improved smoothness, firmness, and moisture content; carrageenans, borage seed oil, squalane, ceramide 3, ceramide 6, red algae extract, dipalmitoyl hydroxyproline and." *U.S. Patent*.
- Crittenden, J. C., R. R. Trussell, D. W. Hand, K. J. Howe, and G. Tchobanoglous. 2012. *MWH's Water Treatment: Principles and Design*. John Wiley & Sons.
- Dahman, Y. 2012. "Optically transparent nanocomposites reinforced with modified biocellulose nanofibers." *Journal of Applied Polymer Science* E188-E196.
- Dai, S., P. Ravi, C. H. Tan, and K. C. Tam. 2004. "Self-assembly behavior of a stimuli-responsive water-soluble [60] fullerene-containing polymer." *Langmuir* 8569-8575.

- Dallinger, R., F. Prosi, H. Segner, and H. Back. 1987. "Contaminated food and uptake of heavy metals by fish: a review and a proposal for further research." *Oecologia* 91-98.
- Dash, J. G. 2012. *Films on solid surfaces: the physics and chemistry of physical adsorption*. Elsevier.
- Davis, A. P., M. Shokouhian, and S. Ni. 2001. "Loading estimates of lead, copper, cadmium, and zinc in urban runoff from specific sources." *Chemosphere* 997-1009.
- Davis, W.M. 2011. *Physical Chemistry: A Modern Introduction*. CRC Press.
- De Nooy, A. E. J., A. C. Besemer, and H. Van Bekkum. 1994. "Highly selective TEMPO mediated oxidation of primary alcohol groups in polysaccharides." *Recueil des Travaux Chimiques des Pays-Bas* 165-166.
- Do, D. D. 1998. *Adsorption analysis: equilibria and kinetics (Vol. 2)*. Imperial College Press.
- Dresselhaus, M. S., G. Dresselhaus, and P. C. Eklund. 1996. *Science of fullerenes and carbon nanotubes: their properties and applications*. Academic press.
- Dreyer, D. R., D. J. Miller, B. D. Freeman, D. R. Paul, and C. W. Bielawski. 2012. "Elucidating the structure of poly (dopamine)." *Langmuir* 6428-6435.

- Duran, N., A. P. Lemes, M. Duran, J. Freer, and J. Baeza. 2011. "A minireview of cellulose nanocrystals and its potential integration as co-product in bioethanol production." *Journal of the Chilean Chemical Society* 672-677.
- El Qada, E. N., S. J. Allen, and G. M. Walker. 2006. "Adsorption of methylene blue onto activated carbon produced from steam activated bituminous coal: a study of equilibrium adsorption isotherm." *Chemical Engineering Journal* 103-110.
- El Qada, E. N., S. J. Allen, and G. M. Walker. 2012. "Polydopamine nanoparticles as a new and highly selective biosorbent for the removal of copper (II) ions from aqueous solutions." *Water, Air, & Soil Pollution* 3535-3544.
- Fischer, E., and A. Speier. 1924. "Darstellung der Ester." *Untersuchungen aus Verschiedenen Gebieten*. 285-291.
- Foo, S. K., and B. H. Hameed. 2010. "Insights into the modeling of adsorption isotherm systems." *Chemical Engineering Journal* 2-10.
- Forman, R. T., and L. E. Alexander. 1998. "Roads and their major ecological effects." *Annual review of ecology and systematics* 207-C2.
- Freundlich, H. M. F. 1906. "Over the adsorption in solution." *J. Phys. Chem* e470.
- Fricke, J., and A. Emmerling. 1992. "Aerogels-Preparation, properties, applications." *Chemistry, Spectroscopy and Applications of Sol-Gel Glasses* 37-87.

- Fu, F., and Q. Wang. 2011. "Removal of heavy metal ions from wastewaters: a review." *Journal of Environmental Management* 407-418.
- Fu, J., Z. Chen, M. Wang, S. Liu, J. Zhang, J. Zhang, R. Han, and Q Xu. 2015. "Adsorption of methylene blue by a high-efficiency adsorbent (polydopamine microspheres): kinetics, isotherm, thermodynamics and mechanism analysis." *Chemical Engineering Journal* 53-61.
- Geckeler, K. E., and S. Samal. 2001. "Rapid assessment of the free radical scavenging property of fullerenes." *Fullerene science and technology* 17-23.
- Giacalone, F., and N. Martin. 2006. "Fullerene polymers: Synthesis and properties." *Chemical reviews* 5136-5190.
- Gregg, S. J., K. S. W. Sing, and H. W. Salzberg. 1967. "Adsorption surface area and porosity." *Journal of The Electrochemical Society* 279C-279C.
- Groot, A. C. 1987. "Contact allergy to cosmetics: causative ingredients." *Contact dermatitis* 26-34.
- Guan, J., X. Chen, T. Wei, F. Liu, S. Wang, Q. Yang, Y. Lu, and S. Yang. 2015. "Directly bonded hybrid of graphene nanoplatelets and fullerene: facile solid-state mechanochemical synthesis and application as carbon-based electrocatalyst for oxygen reduction reaction." *Journal of Materials Chemistry A* 4139-4146.



- Gupta, K. C., and K. Khandekar. 2003. "Acrylamide–methylmethacrylate graft copolymerization onto cellulose using ceric ammonium nitrate." *Journal of Macromolecular Science, Part A* 155-179.
- Gupta, K. C., and K. Khandekar. 2006. "Graft copolymerization of acrylamide onto cellulose in presence of comonomer using ceric ammonium nitrate as initiator." *Journal of applied polymer science* 2546-2558.
- Gupta, K. C., and K. Khandekar. 2002. "Graft copolymerization of acrylamide–methylacrylate comonomers onto cellulose using ceric ammonium nitrate." *Journal of applied polymer science* 2631-2642.
- Gupta, K. C., and K. Khandekar. 2003. "Temperature-responsive cellulose by ceric (IV) ion-initiated graft copolymerization of N-isopropylacrylamide." *Biomacromolecules* 758-765.
- Gupta, K. C., and S. Sahoo. 2001. "Graft copolymerization of acrylonitrile and ethyl methacrylate comonomers on cellulose using ceric ions." *Biomacromolecules* 239-247.
- Habibi, Y., A. L. Goffin, N. Schiltz, E. Duquesne, P. Dubois, and A. Dufresne. 2008. "Bionanocomposites based on poly ( $\epsilon$ -caprolactone)-grafted cellulose nanocrystals by ring-opening polymerization." *Journal of Materials Chemistry* 5002-5010.
- Habibi, Y., L. A. Lucia, and O. J. Rojas. 2010. "Cellulose nanocrystals: chemistry, self-assembly, and applications." *Chemical reviews* 3479-3500.

- Harata, K. 1993. "The X-ray structure of an inclusion complex of heptakis (2, 6-di-O-methyl)- $\beta$ -cyclodextrin with 2-naphthoic acid." *Journal of the Chemical Society, Chemical Communications* 546-547.
- Harkins, W. D. 1952. *The physical chemistry of surface films*. Reinhold.
- Haufler, R. E., J. Conceicao, L. P. F. Chibante, Y. Chai, N. E. Byrne, S. Flanagan, M. M. Haley, S. C. O'Brien, and C. Pan. 1990. "Efficient production of C<sub>60</sub> (buckminsterfullerene), C<sub>60</sub>H<sub>36</sub>, and the solvated buckide ion." *Journal of Physical Chemistry* 8634-8636.
- Hendricks, D. W. 2006. *Water treatment unit processes: physical and chemical*. CRC press.
- Heux, L., G. Chauve, and C. Bonini. 2000. "Nonflocculating and chiral-nematic self-ordering of cellulose microcrystals suspensions in nonpolar solvents." *Langmuir* 8210-8212.
- Ho, Y. S., and G. McKay. 1998. "Kinetic model for lead (II) sorption on to peat." *Adsorption science & technology* 243-255.
- Horsfall, M., A. A. Abia, and A. I. Spiff. 2006. "Kinetic studies on the adsorption of Cd<sup>2+</sup>, Cu<sup>2+</sup> and Zn<sup>2+</sup> ions from aqueous solutions by cassava (*Manihot sculenta* Cranz) tuber bark waste." *Bioresource technology* 283-291.

- Hu, H. C., Y. Liu, and D. D. Zhang. 1999. "Studies on Water-soluble  $\alpha$ -,  $\beta$ -or  $\gamma$ -cyclodextrin Prepolymer Inclusion Complexes with C60." *Journal of inclusion phenomena and macrocyclic chemistry* 295-305.
- Huang, X. D., and S. H. Goh. 2000. "Miscibility of C60-end-capped poly (ethylene oxide) with poly (p-vinylphenol)." *Macromolecular Chemistry and Physics* 2660-2665.
- Hubbe, M. A., O. J. Rojas, L. A. Lucia, and M. Sain. 2008. "Cellulosic nanocomposites: a review." *BioResource* 929-980.
- Hyde, K. D, A. H. Bahkali, and M. A Moslem. 2010. "Fungi - an unusual source for cosmetics." *Fungal Diversity* 1-9.
- Imahori, H., and Y. Sakata. 1997. "Donor-Linked Fullerenes: Photoinduced electron transfer and its potential application." *Advanced Materials* 537-546.
- Inglezakis, V., and S. Pouloupoulos. 2006. *Adsorption, ion exchange and catalysis: design of operations and environmental applications*. Elsevier.
- Jeong, J., J. Jung, M. Choi, J. W. Kim, S. J. Chung, S. Lim, H. Lee, and B. H. Chung. 2012. "Color-Tunable Photoluminescent Fullerene Nanoparticles." *Advanced Materials* 1999-2003.
- Jiang, C. Y. 2014. "A New Approach to Model Adsorption in Heterogeneous Phase System with Monte Carlo Method." *American Journal of Materials Science* 25-38.
- Johnson, R. 1999. "What is that stuff? Lipstick." *Chemical and Engineering News*, 07 12.

- Kalashnikova, I., H. Bizot, P. Bertoncini, B. Cathala, and I. Capron. 2013. "Cellulosic nanorods of various aspect ratios for oil in water Pickering emulsions." *Soft Matter* 952-959.
- Kan, K. H., J. Li, K. Wijesekera, and E. D. Cranston. 2013. "Polymer-grafted cellulose nanocrystals as pH-responsive reversible flocculants." *Biomacromolecules* 3130-3139.
- Kim, S., D. J. Lee, D. S. Kwag, U. Y. Lee, Y. S. Youn, and E. S. Lee. 2014. "Acid pH-activated glycol chitosan/fullerene nanogels for efficient tumor therapy." *Carbohydrate polymers* 692-698.
- Kistler, S. S. 1932. "Coherent expanded-aerogels." *The Journal of Physical Chemistry* 52-64.
- Kokubo, K., K. Matsubayashi, H. Tategaki, H. Takada, and T. Oshima. 2008. "Facile synthesis of highly water-soluble fullerenes more than half-covered by hydroxyl groups." *ACS nano* 327-33.
- Kong, H., C. Gao, and D. Yan. 2004. "Controlled functionalization of multiwalled carbon nanotubes by in situ atom transfer radical polymerization." *Journal of the American Chemical Society* 412-413.
- Kongsricharoern, N., and C. Polprasert. 1995. "Electrochemical precipitation of chromium (Cr 6+) from an electroplating wastewater." *Water Science and Technology* 109-117.

- Korhonen, J. T., M. Kettunen, R. H. Ras, and O. Ikkala. 2011. "Hydrophobic nanocellulose aerogels as floating, sustainable, reusable, and recyclable oil absorbents." *ACS applied materials & interfaces* 1813-1816.
- Kräschmer, W., L. D. Lamb, K. Fostiropoulos, and D. R. Huffman. 1990. "C60: a new form of carbon." *Nature* 354-358.
- Kroto, H. W., J. R. Heath, S. C. O'Brien, R. F. Curl, and R. E. Smalley. 1985. "C 60: buckminsterfullerene." *Nature* 162-163.
- Kumar, S. 2005. "Exploratory analysis of global cosmetic industry: major players, technology and market trends." *Technovation* 1263-1272.
- Kurniawan, T. A., G. Y. Chan, W. H. Lo, and S. Babel. 2006. "Physico-chemical treatment techniques for wastewater laden with heavy metals." *Chemical engineering journal* 83-89.
- Kwag, D. S., K. Park, K. T. Oh, and E. S. Lee. 2013. "Hyaluronated fullerenes with photoluminescent and antitumoral activity." *Chemical Communications* 282-284.
- Lagergren, S. 1898. "About the theory of so-called adsorption of solution substances." *HANDLINGE* 147-156.
- Langmuir, I. 1918. "The adsorption of gases on plane surfaces of glass, mica and platinum." *Journal of the American Chemical society* 1361-1403.

- Laval, C. E. 2011. "Development of Cosmetics." *KTH, School of Chemical Science and Engineering (CHE)*.
- LaVoie, M. J., B. L. Ostaszewski, A. Weihofen, M. G. Schlossmacher, and D. J. Selkoe. 2005. "Dopamine covalently modifies and functionally inactivates parkin." *Nature medicine* 1214-1221.
- Lee, C. I., W. F. Yang, and C. S. Chiou. 2006. "Utilization of water clarifier sludge for copper removal in a liquid fluidized-bed reactor." *Journal of hazardous materials* 58-63.
- Lee, H., B. P. Lee, and P. B. Messersmith. 2007. "A reversible wet/dry adhesive inspired by mussels and geckos." *Nature* 338-341.
- Leung, A. Y., and S. Foster. 1996. *Encyclopedia of common natural ingredients used in food, drugs, and cosmetics (No. Ed. 2)*. John Wiley & Sons, Inc.
- Li, G., Y. Du, Y. Tao, H., Luo, X. Deng, and J. Yang. 2010. "Iron (II) cross-linked chitin-based gel beads: preparation, magnetic property and adsorption of methyl orange." *Carbohydrate Polymers* 706-713.
- Liang, H. W. 2012. "Highly conductive and stretchable conductors fabricated from bacterial cellulose." *NPG Asia Materials* e19.

- Liebscher, J., R. Mrówczyński, H. A. Scheidt, C. Filip, N. D. Hādade, R. Turcu, A. Bender, and S. Beck. 2013. "Structure of polydopamine: a never-ending story?" *Langmuir* 10539-10548.
- Lin, N., J. Huang, and A. Dufresne. 2012. "Preparation, properties and applications of polysaccharide nanocrystals in advanced functional nanomaterials: a review." *Nanoscale* 3274-3294.
- Liu, Y., K. Ai, and L. Lu. 2014. "Polydopamine and its derivative materials: synthesis and promising applications in energy, environmental, and biomedical fields." *Chemical reviews* 5057-5115.
- Ljungberg, N., C. Bonini, F. Bortolussi, C. Boisson, L. Heux, and J. Y. Cavailé 2005. "New nanocomposite materials reinforced with cellulose whiskers in atactic polypropylene: effect of surface and dispersion characteristics." *Biomacromolecules* 2732-2739.
- Ljungberg, N., J. Y. Cavailé and L. Heux. 2006. "Nanocomposites of isotactic polypropylene reinforced with rod-like cellulose whiskers." *Polymer* 6285-6292.
- Lv, Y., H. C. Yang, H. Q. Liang, L. S. Wan, and Z. K. Xu. 2015. "Nanofiltration membranes via co-deposition of polydopamine/polyethylenimine followed by cross-linking." *Journal of Membrane Science* 50-58.
- Lynde, C. W. 2001. "Moisturizers: what they are and how they work." *Skin Therapy Lett* 3-5.

- Mall, I. D., V. C. Srivastava, and N. K. Agarwal. 2006. "Removal of Orange-G and Methyl Violet dyes by adsorption onto bagasse fly ash—kinetic study and equilibrium isotherm analyses." *Dyes and pigments* 69.3 (2006): 210-223. 210-223.
- Mangalam, A. P., J. Simonsen, and A. S. Benight. 2009. "Cellulose/DNA hybrid nanomaterials." *Biomacromolecules* 497-504.
- Mansur, H. S., C. M. Sadahira, A. N. Souza, and A. A. Mansur. 2008. "FTIR spectroscopy characterization of poly (vinyl alcohol) hydrogel with different hydrolysis degree and chemically cross-linked with glutaraldehyde." *Materials Science and Engineering* 539-548.
- Marcus, G. 2009. *Lipstick traces*. Harvard University Press.
- Markovic, Z., and V. Trajkovic. 2008. "Biomedical potential of the reactive oxygen species generation and quenching by fullerenes (C 60)." *Biomaterials* 3561-3573.
- Masel, R. I. 1996. *Principles of adsorption and reaction on solid surfaces*. John Wiley & Sons.
- Maslow, A. H. 1943. "A theory of human motivation." *Psychological review* 370.
- McKay, G., S. J. Allen, I. F. McConvey, and M. S. Otterburn. 1981. "Transport processes in the sorption of colored ions by peat particles." *Journal of Colloid and Interface Science* 323-339.



- McMullan, G., C. Meehan, A. Conneely, N. Kirby, T. Robinson, P. Nigam, I. Banat, R. Marchant, and W. F. Smyth. 2001. "Microbial decolourisation and degradation of textile dyes." *Applied Microbiology and Biotechnology* 81-87.
- Mittal, A., A. Malviya, D. Kaur, J. Mittal, and L. Kurup. 2007. "Studies on the adsorption kinetics and isotherms for the removal and recovery of Methyl Orange from wastewaters using waste materials." *Journal of Hazardous Materials* 229-240.
- Mohammed, N., N. Grishkewich, R. M. Berry, and K. C. Tam. 2015. "Cellulose nanocrystal–alginate hydrogel beads as novel adsorbents for organic dyes in aqueous solutions." *Cellulose* 3725-3738.
- Murthy, C. N., and K. E. Geckeler. 2001. "The water-soluble  $\beta$ -cyclodextrin–[60] fullerene complex." *Chemical Communications* 1194-1195.
- Nagatani, N., K. Fukuda, M. Torizuka, and T. Igarashi. 2002. "Cosmetic composition." *U.S. Patent Application* 475.
- Namasivayam, C., and K. Kadirvelu. 1997. "Agricultural solid wastes for the removal of heavy metals: adsorption of Cu (II) by coirpith carbon." *Chemosphere* 377-399.
- Ngah, W. W., and M. A. K. M. Hanafiah. 2008. "Removal of heavy metal ions from wastewater by chemically modified plant wastes as adsorbents: a review." *Bioresource technology* 3935-3948.
- Noll, K. E. 1991. *Adsorption technology for air and water pollution control*. CRC Press.

- Oura, K., A. V. Zotov, V. G. Lifshits, A. A. Saranin, and M. Katayama. 2003. *Surface science*. Springer.
- Özer, A., D. Özer, and A. Özer. 2004. "The adsorption of copper (II) ions on to dehydrated wheat bran (DWB): determination of the equilibrium and thermodynamic parameters." *Process Biochemistry* 2183-2191.
- Parry, C., and J. Eaton. 1991. "Kohl: a lead-hazardous eye makeup from the Third World to the First World." *Environmental health perspectives* 121.
- Partha, R., and J. L. Conyers. 2009. "Biomedical applications of functionalized fullerene-based nanomaterials." *International journal of nanomedicine* 261.
- Peralta-Videa, J. R., M. L. Lopez, M. Narayan, G. Saupe, and J. Gardea-Torresdey. 2009. "The biochemistry of environmental heavy metal uptake by plants: implications for the food chain." *The international journal of biochemistry & cell biology* 1665-1677.
- Perry, J. H. 1941. *Chemical engineers' handbook*. McGraw-Hill book Company, Incorporated.
- Plum, L. M., L. Rink, and H. Haase. 2010. "The essential toxin: impact of zinc on human health." *International journal of environmental research and public health* 1342-1365.

- Pourjavadi, A., G. R. Mahdavinia, M. J. Zohuriaan-Mehr, and H. Omidian. 2003. "Modified chitosan. I. Optimized cerium ammonium nitrate-induced synthesis of chitosan-graft-polyacrylonitrile." *Journal of Applied Polymer Science* 2048-2054.
- Qiu, H., L. Lv, B. C. Pan, Q. J. Zhang, W. M. Zhang, and Q. X. Zhang. 2009. "Critical review in adsorption kinetic models." *Journal of Zhejiang University Science* 719-724.
- Quinlan, P. J. 2015. "The design and optimization of sustainable biopolymer-based adsorbents for the removal of a model aromatic naphthenic acid from aqueous solution." *Univerisity of Waterloo*.
- Rahman, L., S. Silong, W. M. Zin, M. Z. A. B. Rahman, M. Ahmad, and J. Haron. 2000. "Graft copolymerization of methyl acrylate onto sago starch using ceric ammonium nitrate as an initiator." *Journal of applied polymer science* 516-523.
- Reshetnikov, S. V., S. P. Wasser, I. Duckman, and K. Tsukor. 2000. "Medicinal Value of the Genus Tremella Pers." *International Journal of Medicinal Mushrooms* 2(3).
- Rojas, O. J., G. A. Montero, and Y. Habibi. 2009. "Electrospun nanocomposites from polystyrene loaded with cellulose nanowhiskers." *Journal of Applied Polymer Science* 927-935.
- Romm, S. 1989. "The changing face of beauty." *Aesthetic plastic surgery* 91-98.
- Ross, S., and E. D. Morrison. 1988. *Colloidal systems and interfaces*. John Wiley and Sons.

- Sadeghi, M., and H. Hosseinzadeh. 2010. "Studies on graft copolymerization of 2-hydroxyethylmethacrylate onto kappa-carrageenan initiated by ceric ammonium nitrate." *Journal of the Chilean Chemical Society* 497-502.
- Samal, S., and K. E. Geckeler. 2000. "Cyclodextrin–fullerenes: a new class of water-soluble fullerenes." *Chem. Commun* 1101-1102.
- Samuel, D. F., and M. A. Osman. 2013. *Adsorption processes for water treatment*. Elsevier.
- Sayes, C. M., J. D. Fortner, W. Guo, D. Lyon, A. M. Boyd, K. D. Ausman, Y.J. Tao, et al. 2004. "The differential cytotoxicity of water-soluble fullerenes." *Nano letters* 1881-1887.
- Schaffer, S. E. 2007. "Reading Our Lips: The History of Lipstick Regulation in Western Seats of Power." *Food & Drug LJ* 165.
- Shi, Z., J. Tang, L. Chen, C. Yan, S. Tanvir, W. A. Anderson, Berry M.B., and K. C. Tam. 2015. "Enhanced colloidal stability and antibacterial performance of silver nanoparticles/cellulose nanocrystal hybrids." *Journal of Materials Chemistry B* 603-611.
- Sin, S. L., L. H. Gan, X. Hu, K. C. Tam, and Y. Y. Gan. 2005. "Photochemical and thermal isomerizations of azobenzene-containing amphiphilic diblock copolymers in aqueous micellar aggregates and in film." *Macromolecules* 3943-3948.

- Singh, D. K., and A. R. Ray. 1994. "Graft copolymerization of 2-hydroxyethylmethacrylate onto chitosan films and their blood compatibility." *Journal of applied polymer science* 1115-1121.
- Siqueira, G., J. Bras, and A. Dufresne. 2010. "Cellulosic bionanocomposites: a review of preparation, properties and applications." *Polymers* 728-765.
- Siva, R. 2007. "Status of natural dyes and dye-yielding plants in India." *CURRENT SCIENCE-BANGALORE* 916.
- Stoddart, J. F. 1988. *Host-guest chemistry*. Annual Reports Section" B"(Organic Chemistry), 353-386.
- Sun, X., B. Peng, Y. Ji, J. Chen, and D. Li. 2009. "Chitosan (chitin)/cellulose composite biosorbents prepared using ionic liquid for heavy metal ions adsorption." *AICHE journal* 2062-2069.
- Tam, J., J. Liu, and Z. Yao. 2013. "Effect of microstructure on the antioxidant properties of fullerene polymer solutions." *RSC Adv* 4622-4627.
- Tan, C., B. M. Fung, J. K. Newman, and C. Vu. 2001. "Organic aerogels with very high impact strength." *Advanced materials* 644-646.
- Tang, J., Y. Song, R. M. Berry, and K. C. Tam. 2014. "Polyrhodanine coated cellulose nanocrystals as optical pH indicators." *RSC Advances* 60249-60252.

- Tang, J., Y. Song, S. Tanvir, W. A. Anderson, R. M. Berry, and K. C. Tam. 2015. "Polyrhodanine Coated Cellulose Nanocrystals: A Sustainable Antimicrobial Agent." *ACS Sustainable Chemistry & Engineering* 1801-1809.
- Tapan Kumar, S. 2010. "Adsorption of methyl orange onto chitosan from aqueous solution." *Journal of water resource and protection* 2010.
- Tchounwou, P. B., C. G. Yedjou, A. K. Patlolla, and D. J. Sutton. 2012. "Heavy metal toxicity and the environment." *Molecular, Clinical and Environmental Toxicology* 133-164.
- Temkin, M. I., and V. Pyzhev. 1940. "Kinetics of ammonia synthesis on promoted iron catalysts." *Acta physiochim* 217-222.
- Thompson, B. C., and J. M. Frechet. 2008. "Polymer–fullerene composite solar cells." *Angewandte chemie international edition* 58-77.
- Tian, Y., Y. Cao, Y. Wang, W. Yang, and J. Feng. 2013. "Realizing ultrahigh modulus and high strength of macroscopic graphene oxide papers through cross-linking of mussel-inspired polymers." *Advanced Materials* 2980-2983.
- Topuz, B. B., G. Gündüz, B. Mavis, and Ü. Çolak. 2011. "The effect of tin dioxide (SnO<sub>2</sub>) on the anatase-rutile phase transformation of titania (TiO<sub>2</sub>) in mica-titania pigments and their use in paint." *Dyes and Pigments* 123-128.
- Toth, J. 2002. *Adsorption*. CRC Press.

- Van der Zee, F. P., and S. Villaverde. 2005. "Combined anaerobic–aerobic treatment of azo dyes—a short review of bioreactor studies." *Water research* 1425-1440.
- Wang, X. S., L. F. Chen, F. Y. Li, K. L. Chen, W. Y. Wan, and Y. J. Tang. 2010. "Removal of Cr (VI) with wheat-residue derived black carbon: reaction mechanism and adsorption performance." *Journal of hazardous materials* 816-822.
- Wang, Z., J. Guo, J. Ma, and L. Shao. 2015. "Highly regenerable alkali-resistant magnetic nanoparticles inspired by mussels for rapid selective dye removal offer high-efficiency environmental remediation." *Journal of Materials Chemistry A* 19960-19968.
- Weber, W. J., and J. C. Morris. 1963. "Kinetics of adsorption on carbon from solution." *Journal of the Sanitary Engineering Division* 31-60.
- Wilczak, A., and T. M. Keinath. 1993. "Kinetics of sorption and desorption of copper (II) and lead (II) on activated carbon." *Water Environment Research* 238-244.
- Witkowski, J. A., and L. C. Parish. 2001. "You've come a long way baby: a history of cosmetic lead toxicity." *Clinics in dermatology* 367-370.
- Woignier, T., J. Phalippou, and J. Zarzycki. 1984. "Monolithic aerogels in the systems  $\text{SiO}_2$  B<sub>2</sub>O<sub>3</sub>,  $\text{SiO}_2$  P<sub>2</sub>O<sub>5</sub>,  $\text{SiO}_2$  B<sub>2</sub>O<sub>3</sub> P<sub>2</sub>O<sub>5</sub>." *Journal of Non-Crystalline Solids* 117-130.

- Wong, K. K., et al. 2003. "Removal of Cu and Pb from electroplating wastewater using tartaric acid modified rice husk." *Process Biochemistry* 437-445.
- Wu, C., H. Wang, Z. Wei, C. Li, and Z. Luo. 2015. "Polydopamine-mediated surface functionalization of electrospun nanofibrous membranes: Preparation, characterization and their adsorption properties towards heavy metal ions." *Applied Surface Science* 207-215.
- Wu, J., L. B. Alemany, W. Li, L. Petrie, C. Welker, and J. D. Fortner. 2014. "Reduction of hydroxylated fullerene (fullerol) in water by zinc: Reaction and hemiketal product characterization." *Environmental science & technology* 7384-7392.
- Wu, Y. S., H. K. Lee, and S. F. Y. Li. 2001. "High-performance chiral separation of fourteen triazole fungicides by sulfated  $\beta$ -cyclodextrin-mediated capillary electrophoresis." *Journal of chromatography* 171-179.
- Wu, Z. Y., C. Li, H. W. Liang, J. F. Chen, and S. H. Yu. 2013. "Ultralight, flexible, and fire-resistant carbon nanofiber aerogels from bacterial cellulose." *Angewandte Chemie* 2997-3001.
- Xiong, S., F. Yang, H. Jiang, J. Ma, and X. Lu. 2006. "Adsorption of antimony on IOCS: kinetics and mechanisms." *Acta Scientiae Circumstantiae* 607-612.
- Xiong, S., F. Yang, H. Jiang, J. Ma, and X. Lu. 2012. "Covalently bonded polyaniline/fullerene hybrids with coral-like morphology for high-performance supercapacitor." *Electrochimica Acta* 235-242.



- Yang, Y., Z. Wei, C. Wang, and Z. Tong. 2013. "Lignin-based Pickering HIPEs for macroporous foams and their enhanced adsorption of copper (II) ions." *Chemical Communications* 7144-7146.
- Yao, W.F., H. Wang, X.H. Xu, X.F. Cheng, J. Huang, S.X. Shang, X.N. Yang, and M. Wang. 2003. "Photocatalytic property of bismuth titanate Bi<sub>2</sub>TiO<sub>5</sub> crystals." *Applied Catalysis A: General* 185-190.
- Yao, Z., and J. H. Tam. 2014. "Fullerene-derived cellulose nanocrystal, their preparation and uses thereof." *U.S. Patent Application* 999.
- Yao, Z., and K. C. Tam. 2011. "Stimuli-Responsive Water-Soluble Fullerene (C<sub>60</sub>) Polymeric Systems." *Macromolecular rapid communications* 1863-1885.
- Yu, Y., J. G. Shapter, R. Popelka-Filcoff, J. W. Bennett, and A. V. Ellis. 2014. "Copper removal using bio-inspired polydopamine coated natural zeolites." *Journal of hazardous materials* 174-182.
- Yuan, H., Y. Nishiyama, M. Wada, and S. Kuga. 2006. "Surface acylation of cellulose whiskers by drying aqueous emulsion." *Biomacromolecules* 696-700.
- Zeldowitsch, J. 1934. "Über den mechanismus der katalytischen oxydation von CO an MnO<sub>2</sub>." *Acta physicochim* 364-449.

- Zeng, T., H. Y. Niu, Y. R. Ma, W. H. Li, and Y. Q. Cai. 2013. "In situ growth of gold nanoparticles onto polydopamine-encapsulated magnetic microspheres for catalytic reduction of nitrobenzene." *Applied Catalysis B: Environmental* 134, 26-33.
- Zhang, G., R Qu, C. Sun, C. Ji, H. Chen, C. Wang, and Y. Niu. 2008. "Adsorption for metal ions of chitosan coated cotton fiber." *Journal of applied polymer science* 2321-2327.
- Zhang, L. F., J. L. Zhao, X. Zeng, L. Mu, X. K. Jiang, M. Deng, J.X. Zhang, and G. Wei. 2011. "Tuning with pH: The selectivity of a new rhodamine B derivative chemosensor for Fe<sup>3+</sup> and Cu<sup>2+</sup>." *Sensors and Actuators B: Chemical* 662-669.
- Zhang, Z., J. Zhang, B. Zhang, and J. Tang. 2013. "Mussel-inspired functionalization of graphene for synthesizing Ag-polydopamine-graphene nanosheets as antibacterial materials." *Nanoscale* 118-123.
- Zhao, J., X. Zhang, X. He, M. Xiao, W. Zhang, and C. Lu. 2015. "A super biosorbent from dendrimer poly (amidoamine)-grafted cellulose nanofibril aerogels for effective removal of Cr (VI)." *Journal of Materials Chemistry A* 14703-14711.
- Zhao, J., X. Zhang, X. He, M. Xiao, W. Zhang, and C. Lu. 2012. "Microstructure, rheology, and potential oil absorbency of poly (butyl methacrylate) and poly (hydroxyethyl methacrylate) blends." *Journal of Macromolecular Science, Part B* 2297-2309.
- Zheng, G., and H. D. Stöver. 2002. "Grafting of poly (alkyl (meth) acrylates) from swellable poly (DVB80-co-HEMA) microspheres by atom transfer radical polymerization." *Macromolecules* 7612-7619.